



Fitting SDE models to nonlinear Kac–Zwanzig heat bath models

R. Kupferman^{a,*}, A.M. Stuart^b

^a *Institute of Mathematics, The Hebrew University, Jerusalem 91904, Israel*

^b *Mathematics Institute, University of Warwick, Coventry CV4 7AL, UK*

Received 18 December 2002; received in revised form 28 October 2003; accepted 6 April 2004

Communicated by I. Mezic

Abstract

We study a class of “particle in a heat bath” models, which are a generalization of the well-known Kac–Zwanzig class of models, but where the coupling between the distinguished particle and the n heat bath particles is through nonlinear springs. The heat bath particles have random initial data drawn from an equilibrium Gibbs density. The primary objective is to approximate the forces exerted by the heat bath—which we do not want to resolve—by a stochastic process. By means of the central limit theorem for Gaussian processes, and heuristics based on linear response theory, we demonstrate conditions under which it is natural to expect that the trajectories of the distinguished particle can be weakly approximated, as $n \rightarrow \infty$, by the solution of a Markovian SDE. The quality of this approximation is verified by numerical calculations with parameters chosen according to the linear response theory. Alternatively, the parameters of the effective equation can be chosen using time series analysis. This is done and agreement with linear response theory is shown to be good.

© 2004 Elsevier B.V. All rights reserved.

PACS: 05.40.–a; 05.45.–a; 02.50.–r

Keywords: Hamiltonian systems; Heat bath; Stochastic differential equations; Nonlinear oscillators

1. Introduction

Mechanical models for particles immersed in a heat bath have a long history, dating back to the 1960s with the model of Ford et al. [1]. The simplest models consist of a “distinguished” particle interacting with a large collection of n “heat bath” particles [2,3]. The initial conditions for the heat bath particles are assumed to be random, with a dis-

* Corresponding author. Present address: Department of Mathematics, Lawrence Berkeley Laboratory, MS 50A-1148, Berkeley CA 94720, USA.

E-mail addresses: raz@math.huji.ac.il (R. Kupferman); stuart@maths.warwick.ac.uk (A.M. Stuart).

URL: <http://www.math.huji.ac.il/~razk> (R. Kupferman); <http://www.maths.warwick.ac.uk/~stuart> (A.M. Stuart)..

tribution governed by the laws of statistical physics. Such models have recently been studied as test problems for dimensional reduction methods such as coarse time-stepping [4–6], optimal prediction [7,8], and transfer operators [9].

In a recent publication [10] we analyzed the $n \rightarrow \infty$ limit of a variant of the Kac–Zwanzig model. On bounded time intervals the behaviour of the distinguished particle was proved to be weakly approximated by a (generalized) Langevin stochastic differential equation (SDE). While this weak approximation was not proved for infinite time intervals, the long time behaviour of the distinguished particle’s trajectories was found numerically to resemble that of the limiting SDE: the close relationship between the large system of ordinary differential equations (ODEs) and the limiting SDE over large times is manifest, for example, in the good agreement in the empirical measures and auto-covariance functions of the two processes.

All the above analyses use explicitly the simplicity of the Kac–Zwanzig model and, notably, the fact that the distinguished particle interacts with the heat bath particles through linear springs. Using standard methods for linear ODEs one can then eliminate the heat bath variables and obtain, in explicit form, a closed integro-differential equation for the distinguished particle; this facilitates analysis of the $n \rightarrow \infty$ limit. The form of Hamiltonians which we study in this paper are given by

$$H(P_n, Q_n, p, q) = \frac{P_n^2}{2} + V(Q_n) + \sum_{j=1}^n \left[\frac{p_j^2}{2m_j} + k_j v(q_j - Q_n) \right], \quad (1)$$

where (P_n, Q_n) are the momentum and position of the distinguished particle, and the remaining (p_j, q_j) are the momenta and positions of the heat bath. The work of Kac and Zwanzig which laid the foundation of this subject area concerns the case of quadratic (Hookean) potential v . Here we consider more general non-Hookean potentials, in particular quartic ones, and again consider $n \gg 1$. At the end of this section we describe other forms of nonlinear coupling, different from (1), that arise in the literature.

The purpose of this paper is to obtain understanding of such nonlinear bath-particle coupling. In particular we investigate the approximation of the motion of the distinguished particle by an SDE, using a combination of rigorous analysis, formal asymptotics and time series analysis. It is hoped that the insight we obtain here will inform more ambitious projects to fit SDEs to coarse models of molecular conformational dynamics such as that initiated in [11]. Where conformational transitions are exceptionally rare events, it may be impossible to generate sufficiently long sample paths of the ODEs to fit SDEs which are valid on the whole phase space; but it may still be useful to fit them locally, within a conformation and this idea is one considered in [11]. Furthermore, the techniques introduced here may also, in principle, be used to fit experimental data.

A recent publication which investigates the possibility of dimension reduction through stochastic closure is [12]. That work exploits a time scale separation to facilitate the dimension reduction and applications are drawn from the atmospheric sciences. Here we exploit the broad spectrum of the heat bath.

We start by considering a single nonlinear oscillator with initial data drawn from a Gibbs distribution (Section 2.1). For power law potentials the general solution can be related to a normalized solution via a similarity transformation. We then consider a collection of n such oscillators, varying in mass and spring coefficient, and analyze the (time-dependent) force, $F_n(t)$, that they exert on their common anchor point (Section 2.2). This force is a random function in the probability space induced by the initial data. For masses and spring coefficients satisfying certain properties we prove that $F_n(t)$ converges, as $n \rightarrow \infty$, to a Gaussian process, $F(t)$, with zero mean and a computable auto-covariance. The convergence is in distribution, i.e., weak convergence [13], in the space of continuous functions $C([0, T_0], \mathbb{R})$, where T_0 is finite but arbitrary. By fitting numerical data, we find parameters for which the auto-covariance of the limiting process is well approximated by an exponential decay, i.e., the limiting process closely resembles an Ornstein–Uhlenbeck (OU) process (Section 2.3). Then we use methods from time series analysis to fit OU processes to data generated at finite n , comparing the results with the fits obtained at $n = \infty$, and showing good agreement (Section 2.4). The results of Section 2 are generalizable to arbitrary potentials without power law form and this is discussed in Section 2.5.

The next step is to analyze the force exerted by an oscillator when the anchor point is moving (Section 3.1). The expected value of this force is called “drag”, whereas the deviation from the mean is called “noise”. In general,

the drag depends on the entire history of the motion of the anchor point via a memory kernel. For linear springs the separation between drag and noise follows immediately from the variation of constants formula. For nonlinear springs these components cannot be obtained analytically. We perform a perturbative expansion in the limit where the displacement of the anchor point is small and obtain a “linear response” solution, where the drag force is given by the velocity of the anchor point convolved with a memory kernel. This memory kernel is proportional to the auto-covariance of the fluctuating force at equilibrium (when the anchor point is static—Section 2.2), which is a manifestation of the fluctuation–dissipation principle. Numerical computations are used to extend this analysis by showing a deviation from linear response when the displacement of the anchor point is not small (Section 3.2). It is also demonstrated numerically that increasing the temperature improves the accuracy of the linear response approximation. Related discussion about the validity of linear response theory may be found in [14,15]; there the effects of chaotic mixing, and of system dimension, are explored.

Finally in Section 4.1 we return to the full Hamiltonian problem (1) for a particle interacting through nonlinear springs with a collection of n heat bath oscillators. The analysis in Section 3.1, as well as the analysis in the case of linear bath-particle coupling, suggests how to construct an approximate generalized Langevin equation in the linear response regime. When the equilibrium fluctuations behave like an OU process, it is possible to eliminate the memory by the introduction of one auxiliary variable, and obtain an SDE. First we use linear response theory to fit parameters in this SDE and good agreement with the Hamiltonian system is shown. Secondly we use time series analysis to find the optimal parameter fit of this SDE to the motion of the distinguished particle in the full Hamiltonian problem. Agreement between the parameter estimates, and those obtained by linear response theory, is good. Hence the resulting SDE approximates well, in a weak sense, the trajectories of the distinguished particle for large n (Sections 4.2 and 4.3).

Concluding discussions are given in Section 5.

Earlier work by Lindenberg and co-workers study particle-bath couplings induced by Hamiltonians of the form

$$H(P_n, Q_n, p, q) = \frac{P_n^2}{2} + V(Q_n) + \sum_{j=1}^n \left[\frac{p_j^2}{2m_j} + k_j(q_j - a_j(Q_n))^2 \right] \quad (2)$$

and of the form

$$H(P_n, Q_n, p, q) = \frac{P_n^2}{2} + V(Q_n) + \sum_{j=1}^n \left[\frac{p_j^2}{2m_j} + k_j q_j^2 / 2 \right] - \lambda Q_n \Gamma(q), \quad (3)$$

where $q = (q_1, \dots, q_n)$. The Hamiltonian (2) is studied in [16], with later work in cosmology in [17]; the quadratic coupling potential allows explicit elimination of the bath variables. The Hamiltonian (3) is studied in [18]; perturbation techniques are applied, making the assumption that λ is small and that Γ is polynomial in q . Classical models that use nonlinear springs to induce coupling between the distinguished particle and the heat bath have been also studied numerically [5].

Models that use nonlinear interactions between distinguished particles and heat baths have also been studied in the quantum mechanical context; indeed some of the references in the previous paragraph include the quantum case. Classical models are limits of quantum models, and are treated in many cases quasi-classically [19]. In [20] a quantum system is analyzed via the derivation of a master equation for the system’s density operator. In these two papers, the nonlinearity is treated by perturbative expansions, and in this respect differ from the present work.

2. Construction of random functions with nonlinear oscillators

In this section we show that sums of solutions of a single degree of freedom Hamiltonian system with random data can be approximated by Gaussian processes. We also show that, in certain regimes, these limiting Gaussian

processes can themselves be approximated by OU processes. Section 2.1 introduces the prototypical Hamiltonian we study—separable with quartic potential. Section 2.2 proves convergence of sums of n solutions to this problem, with canonical initial data, to Gaussian processes. Section 2.3 contains numerical validation of the theory and studies the approximation of the limiting ($n = \infty$) Gaussian process by an OU process. This is taken further in Section 2.4 where a systematic time series analysis is undertaken to fit OU processes to data generated by the finite ($n < \infty$) sum of nonlinear oscillators. Section 2.5 contains generalization to potentials other than quartic.

2.1. A nonlinear oscillator with random initial data

Consider the following single degree of freedom Hamiltonian

$$H(p, q) = \frac{p^2}{2m} + \frac{kq^4}{4}, \quad (4)$$

where p and q are momentum and coordinate. This Hamiltonian describes a particle (or an oscillator) of mass m in a quartic potential well, $v(q) = (1/4)kq^4$. Hamilton's equations are

$$\dot{q} = \frac{p}{m}, \quad q(0) = q_0, \quad \dot{p} = -kq^3, \quad p(0) = p_0, \quad (5)$$

where (p_0, q_0) are the initial data. The initial conditions are assumed to be random, drawn from the Gibbs distribution with density $Z^{-1} \exp[-\beta H(p_0, q_0)]$, where Z is a normalization factor and β the inverse temperature. For $H(p, q)$ given by (4) p_0 and q_0 are independent, and their joint probability density is $f(p_0, q_0)$, where

$$f(p, q) = \frac{\beta^{1/2}}{(2\pi m)^{1/2}} \exp\left(-\frac{\beta p^2}{2m}\right) \cdot \frac{(4\beta k)^{1/4}}{\Gamma(1/4)} \exp\left(-\frac{\beta k q^4}{4}\right) \quad (6)$$

and $\Gamma(x)$ is the Gamma function [21]. Note, however, that although the initial data is random, most of the parameter estimation that we perform in this section, and subsequent ones, is based on a single path of the underlying dynamics, generated by a single pick of the initial data.

Eq. (5) satisfies a homogeneity property: its general solution can be expressed in terms of the solution of a “normalized” equation. Let $\Phi(t)$ be the solution of the initial value problem:

$$\ddot{\Phi} + \Phi^3 = 0, \quad \Phi(0) = 1, \quad \dot{\Phi}(0) = 0, \quad (7)$$

then the solution to (5) is

$$q(t) = k^{-1/4} \xi_0 \Phi(\xi_0 \nu t + \tau_0), \quad (8)$$

where $\nu = k^{1/4} m^{-1/2}$. The parameters ξ_0 and τ_0 are related to the initial data by

$$q_0 = k^{-1/4} \xi_0 \Phi(\tau_0), \quad p_0 = m^{1/2} \xi_0^2 \dot{\Phi}(\tau_0). \quad (9)$$

It is readily verified that $\Phi(t)$ is periodic with period, to five significant digits:

$$T = \pi^{-1/2} [\Gamma(\frac{1}{4})]^2 = 7.4163$$

and satisfies the normalized energy conservation relation:

$$2\dot{\Phi}^2(t) + \Phi^4(t) = 1. \quad (10)$$

The relation (9) defines a mapping from the original variables (p, q) to action-angle-like variables (ξ, τ) . Viewed as a map

$$(\xi, \tau) \in \mathbb{R} \times [0, T] \rightarrow (q, p) \in \mathbb{R}^2,$$

the mapping is onto and takes two points in the domain into every point in its range (the mapping is one-to-one and onto if we restrict ξ to \mathbb{R}^+). In particular, the density (6) induces a density on (ξ, τ) , as established by the following proposition.

Proposition 2.1. *The density (6) induces the following density on (ξ, τ) :*

$$\tilde{f}(\xi, \tau) = m^{1/2} k^{-1/4} \xi^2 f(p, q) = \frac{\beta^{3/4}}{\sqrt{\pi} \Gamma(1/4)} \xi^2 \exp\left(-\frac{\beta \xi^4}{4}\right). \tag{11}$$

That is, τ and ξ are independent, τ is uniformly distributed in $[0, T]$ and ξ has a density proportional to $\xi^2 \exp(-\beta \xi^4/4)$ on \mathbb{R} .

We refer to phases and amplitudes distributed this way as *canonical*.

Proof. The change of variables formula is

$$\tilde{f}(\xi, \tau) = \frac{f(p(\xi, \tau), q(\xi, \tau))}{|J(\xi, \tau)|},$$

where

$$|J(\xi, \tau)|^{-1} = \begin{vmatrix} \frac{\partial p}{\partial \xi} & \frac{\partial p}{\partial \tau} \\ \frac{\partial q}{\partial \xi} & \frac{\partial q}{\partial \tau} \end{vmatrix} = m^{1/2} k^{-1/4} \xi^2 [2\dot{\Phi}^2(\tau) - \Phi(\tau)\ddot{\Phi}(\tau)] = m^{1/2} k^{-1/4} \xi^2$$

and we have used (7) and (10). □

2.2. Sums of nonlinear oscillations

We consider now n independent oscillators with interaction potentials $(1/4)k_j q^4$ and masses m_j ; this determines the frequencies $\nu_j, j = 1, 2, \dots, n$ through $\nu_j = k_j^{1/4} m_j^{-1/2}$. Each oscillator has random initial data (ξ_j, τ_j) , which are mutually independent sequences of i.i.d. random variables. The phase variables τ_j have uniform distribution $\mathcal{U}[0, T]$, whereas the action-like variables ξ_j have density proportional to $\xi^2 \exp(-\beta \xi^4/4)$. The oscillators then have position $q_j(t)$ determined by (8). The joint force that these oscillators exert on the common anchor point (the origin) is given by the sum over derivatives of the potential, that is

$$Y_n(t) = \sum_{j=1}^n k_j q_j^3(t) = \sum_{j=1}^n k_j^{1/4} \xi_j^3 \Phi^3(\xi_j \nu_j t + \tau_j). \tag{12}$$

We are interested in the limiting behaviour of such sums as $n \rightarrow \infty$. Some assumptions need to be made for the parameters k_j and ν_j which, together, determine the m_j . The ν_j determine the characteristic frequencies of the oscillators once the ξ_j are known, i.e. they determine the “spectrum of the heat bath”. Note, however, that the actual spectrum in (12) is also amplitude (i.e., ξ) dependent. Since heat baths are characterized by broad and dense

spectra, we want the set of ν_j to cover an increasingly large range of frequencies, in an increasingly dense manner, as $n \rightarrow \infty$. A simple choice that satisfies this requirement is

$$\nu_j = j \Delta \nu, \quad \Delta \nu = \frac{n^a}{n} \tag{13}$$

for some $a \in (0, 1)$. This choice differs from the one used in [10], where the analogous parameter was chosen at random. Because the frequency is amplitude dependent here, and the amplitude is a random variable, there is sufficient randomness in the spectrum even if the ν_j are chosen equi-distant.

In addition we make the following assumption for the distribution of coefficients k_j .

Assumption 2.1. *The coefficients k_j can be written as*

$$k_j^{1/2} = g(\nu_j) \Delta \nu,$$

where $g(\nu)$ is uniformly bounded on \mathbb{R}^+ and satisfies $g(\nu) \leq c/\nu^{1+b}$ for some $b > 0$.

Note that this implies that the masses have the form

$$m_j = \frac{g(j\Delta \nu)}{j^2 \Delta \nu}.$$

We may now formulate a theorem concerning the limiting behaviour of (12).

Theorem 2.1. *Let $Y_n(t)$ be a sequence of random functions given by (12) with ν_j given by (13), k_j satisfying Assumption 2.1 and canonical τ_j, ξ_j . Then $Y_n \Rightarrow Y$ in $C([0, T_0], \mathbb{R})$, $T_0 > 0$ arbitrary, where $Y(t)$ is a stationary Gaussian process with mean zero and auto-covariance*

$$\sigma(t) = \beta^{-3/2} \int_0^\infty g(\nu) h(\beta^{-1/4} \nu t) d\nu, \tag{14}$$

here $h(t)$ is the auto-covariance of the force exerted by a single oscillator with canonical data and unit parameters $m = k = \beta = 1$:

$$h(t) = \frac{1}{\sqrt{2}\Gamma(3/4)} \int_{-\infty}^\infty \xi^8 e^{-\xi^4/4} \left[\frac{1}{T} \int_0^T \Phi^3(\xi t + \tau) \Phi^3(\tau) d\tau \right] d\xi. \tag{15}$$

Proof. The proof relies on the following theorem ([22], p. 450). Let Y_n be a collection of real-valued almost-surely continuous stochastic processes on $[0, T_0]$, such that:

- (1) The finite-dimensional distributions of Y_n weakly converge to those of an almost-surely continuous process Y .
- (2) Tightness: there exist positive constants α, η, M such that for all n

$$\mathbb{E}|Y_n(t+u) - Y_n(t)|^\alpha \leq M |u|^{1+\eta}.$$

(Here \mathbb{E} denotes expectation with respect to the random data on (ξ, τ) .) Then $Y_n \Rightarrow Y$ in $C([0, T_0], \mathbb{R})$.

The weak convergence of the finite-dimensional distributions is proved in Appendix A in Lemma A.1. The tightness property is proved in Lemma A.2. □

Comments:

- (1) The auto-covariance of the force exerted by an oscillator with parameters k, m , and β is

$$\sigma_1(t) = \beta^{-3/2} k^{1/2} h(\beta^{-1/4} \nu t), \tag{16}$$

where $v = k^{1/4}m^{-1/2}$. The finite n auto-covariance is then

$$\sigma_n(t) = \mathbb{E}Y_n(s)Y_n(s + t) = \beta^{-3/2} \sum_{j=1}^n g(v_j)h(\beta^{-1/4}v_j t) \Delta v, \tag{17}$$

where we have used Assumption 2.1 for the form of the k_j . The limit $n \rightarrow \infty$ gives (14).

The deviation of $\sigma_n(t)$ from $\sigma(t)$ has two contributions: the approximation of the integral (14) by quadrature, and the truncation of the upper limit of integration at $v = n^a$. The dependence of these two contributions on n depends on specific properties of the functions $g(v)$ and $h(t)$.

- (2) The inverse temperature β scales both the magnitude and the timescale of the auto-covariance: the larger the temperature is, the larger and faster are the force fluctuations. This is a manifestation of the underlying nonlinearity. The precise scaling is however a characteristic of the quartic potential.
- (3) The function $h(t)$, which is the auto-covariance of the force exerted by a single oscillator with unit parameters, is bounded and $h(t) \sim t^{-1}$ as $t \rightarrow \infty$. To see this we note that (15) is of the form

$$h(t) = \lim_{M \rightarrow \infty} \int_{-M}^M \xi^8 e^{-\xi^4/4} \phi(\xi t) d\xi,$$

where ϕ is continuous, T -periodic and averages to zero over a period; hence ϕ is bounded and thus h is bounded. Integrating by parts, we find

$$h(t) = \lim_{M \rightarrow \infty} \frac{1}{t} \int_{-M}^M (\xi^{11} - 8\xi^7) e^{-\xi^4/4} \psi(\xi t) d\xi,$$

where $\psi(x) = \int_0^x \phi(x') dx'$ is bounded; the integral can be bounded uniformly in t and $|h(t)| \leq C/t$. Thus, for every fixed n , the auto-covariance of Y_n tends to zero in time.

- (4) Together with Assumption 2.1, the boundedness of $h(t)$ and the decay estimate for $h(t)$ show that $\sigma(t)$ given by (14) satisfies $|\sigma(t)| \leq C \log(t)/t$.¹ Hence the auto-covariance of Y tends to zero as $t \rightarrow \infty$. Item 3 and Eq. (17) show that the auto-covariance of Y_n also tends to zero as $t \rightarrow \infty$.
- (5) In the case of linear bath-particle coupling (see [10]) the situation is different, if we consider the auto-covariance found for fixed k_j, m_j (and hence v_j) and averaged over random data. The force exerted by n oscillators with masses m_j , spring constants k_j , and Gibbsian initial data is

$$Y_n(t) = \sum_{j=1}^n k_j^{1/2} \xi_j \cos(v_j t + \tau_j),$$

where $v_j = (k_j/m_j)^{1/2}$, and ξ_j, τ_j are mutually i.i.d. sequences $\xi_j \sim \beta^{-1/2} \mathcal{N}(0, 1)$ and $\tau_j \sim \mathcal{U}(0, 2\pi)$. Letting $k_j = g(v_j)\Delta v$, with $v_j \sim \mathcal{U}(0, n^a)$ i.i.d and Assumption 2.1 on g , we get the finite n auto-covariance

$$\sigma_n(t) = \mathbb{E}Y_n(s)Y_n(s + t) = \beta^{-1} \sum_{j=1}^n g(v_j)h(v_j t)\Delta v,$$

where $h(t) = (1/2) \cos(t)$. (Again \mathbb{E} is expectation only with respect to random data.) This function is quasi-periodic and does not decay in time for any finite n . However, in the limit $n \rightarrow \infty$, we obtain

¹ To prove this, write (14) in terms of $s = vt$ and split the interval into $(0, \log(t))$, $(\log(t), t)$ and (t, ∞) .

$$\sigma(t) = \beta^{-1} \int_0^\infty g(v)h(vt) \, dv.$$

This function can decay in time for appropriate choices of g . Note the contrast with the nonlinear case where both the finite and infinite n auto-covariances decay in time.

- (6) Note, however, that the empirical auto-covariance, found by averaging over time, will not decay to zero for either the linear or nonlinear heat baths at finite n . It is this auto-covariance which we calculate numerically in Fig. 5 below.
- (7) The extension of these results to other power-law valued potentials is straightforward. More general potentials are treated in Section 2.5.

2.3. Comparison of limiting process and OU process

We have proved that the random functions $Y_n(t)$, defined by (12), weakly converge to a stationary Gaussian process $Y(t)$ of mean zero and auto-covariance $\sigma(t)$ given by (14). We next validate this result numerically by studying $Y_n(t)$, n large, obtained by an explicit construction of the sum (12) with random data for ξ_j, τ_j .

The limiting auto-covariance, $\sigma(t)$, depends on $h(t)$, which is a property of the shape of the potential $v(q) = q^4/4$, and on $g(v)$, which is a characteristic of the heat bath parameters. In Fig. 1 we plot $h(t)$, given by (15), which was obtained by a direct numerical integration; this function exhibits damped oscillations.

Every choice of $g(v)$ that satisfies Assumption 2.1 yields a different $\sigma(t)$. In view of the β dependence in (14), if we write $\sigma = \sigma(t; \beta)$ to emphasize the β dependence, then

$$\sigma(t; \beta) = \beta^{-3/2} \sigma(\beta^{-1/4}t; 1)$$

and hence it is sufficient to calculate $\sigma(t; \beta)$ for $\beta = 1$. Of particular interest are parameters for which the auto-covariance is close to exponential. In this case the limiting process can be approximated by an Ornstein–Uhlenbeck process. Graphs of $\sigma(t)$ that correspond to $\beta = 1$ and $g(v)$ of the form

$$g(v) = \frac{\mu}{\mu^2 + v^2} \tag{18}$$

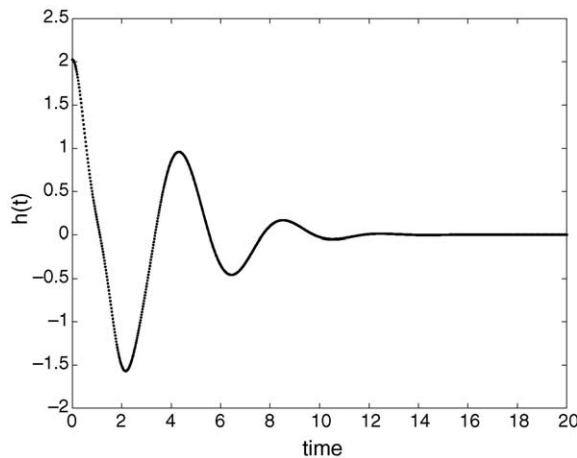


Fig. 1. The function $h(t)$ given by (15).

are displayed in Fig. 2. Each curve is fitted, using a nonlinear least squares fit, to an exponential function:

$$\sigma(t) \approx \beta_0^{-1} e^{-\alpha_0 t}. \tag{19}$$

(See [23] for similar fits of components of deterministic systems to OU processes.) For $\mu = 0.4$, for example, an excellent exponential fit (19) is obtained with $\beta_0^{-1} = 3.108$ and $\alpha_0 = 0.623$; this estimate was obtained by applying the nonlinear least square fit using data from the time interval $t \in [0, 2]$; this is roughly the length of the characteristic decay time of $\sigma(t)$. Putting back temperature dependence we have

$$\beta_0^{-1} = 3.108\beta^{-3/2}, \quad \alpha_0 = 0.623\beta^{-1/4}. \tag{20}$$

This suggests that $Y_n(t)$ is well-approximated, for $n \gg 1$, by the stationary OU process, $U(t)$, defined by

$$dU = -\alpha_0 U dt + (2\alpha_0\beta_0^{-1})^{1/2} dB, \quad U(0) \sim \mathcal{N}(0, \beta_0^{-1}), \tag{21}$$

where $B(t)$ is standard Brownian motion. Note that the OU temperature β_0^{-1} differs from the temperature β^{-1} associated with the Gibbs distribution; it does not even scale linearly with β^{-1} .

In order to speed up numerical simulations, it is of interest to determine the value of a for which the convergence rate of Y_n is optimal. Such a calculation was carried out analytically for linear springs in [10], yielding $a = 1/3$. Here we estimate the optimal value of a by minimizing the L^2 -norm of the error in $\sigma(t)$:

$$\text{Err}(a) = \left\| \int_0^\infty g(v)h(vt) dv - \sum_{j=1}^n g(v_j)h(v_j t) \Delta v \right\|_2.$$

If we assume that $h(t)$ decays like $1/t$ and balance the error from truncating the infinite integral to $[0, n^a)$ with the error from quadrature we obtain $a = 1/4$ as the optimal value. This value was used in all the calculations shown in this paper.

We proceed to compare the processes $Y_n(t)$, with $g(v)$ given by (18) and $\mu = 0.4$, with the OU process $U(t)$ given by (21). In Fig. 3 we plot a sample path of $Y_n(t)$ for $n = 20,000$ and $\beta = 1$. For comparison, we plot a sample path of the limiting OU process. One approach to quantifying the similarity manifest in this figure is to make statistical comparisons between ensembles of solutions of both processes on a bounded time interval. However, the long term results in [10] suggest that it is also of interest to compare the long term statistics of single trajectories and this is what we do here.

In Fig. 4 we display sample path empirical distributions of $Y_n(t)$, calculated with $a = 1/4$ and $\beta = 1$. The distributions are compared with the empirical distribution of $U(t)$, which is a Gaussian with variance β_0^{-1} . For $n = 500$ the empirical distribution still varies noticeably from one realization to another, deviating from the approximate limiting distribution of the OU process (21). For $n = 20,000$ the statistical errors are significantly smaller, and the empirical distribution of $Y_n(t)$ is close to the empirical distribution of the approximating process. Recall that the fit to an OU process is performed at the $n = \infty$ limit.

In Fig. 5 we show the empirical auto-covariances for the same sample paths of $Y_n(t)$, which we compare to the auto-covariance (19) of $U(t)$. Here too, the data is very scattered about the approximate limiting behaviour when $n = 500$. It is much less so when $n = 20,000$ where the fit to the approximating SDE is excellent.

2.4. Time series analysis

To test the robustness of the approximation of $Y_n(t)$ by an OU process, we fit $Y_n(t)$ to an OU process using parameter estimation techniques from time series analysis. In addition to being a consistency check on the ad hoc data fitting from the previous section, the approach we use in this section is likely to be the most practical approach when model parameters cannot be obtained by analytical means. It also forms a rational basis for hypothesis testing.

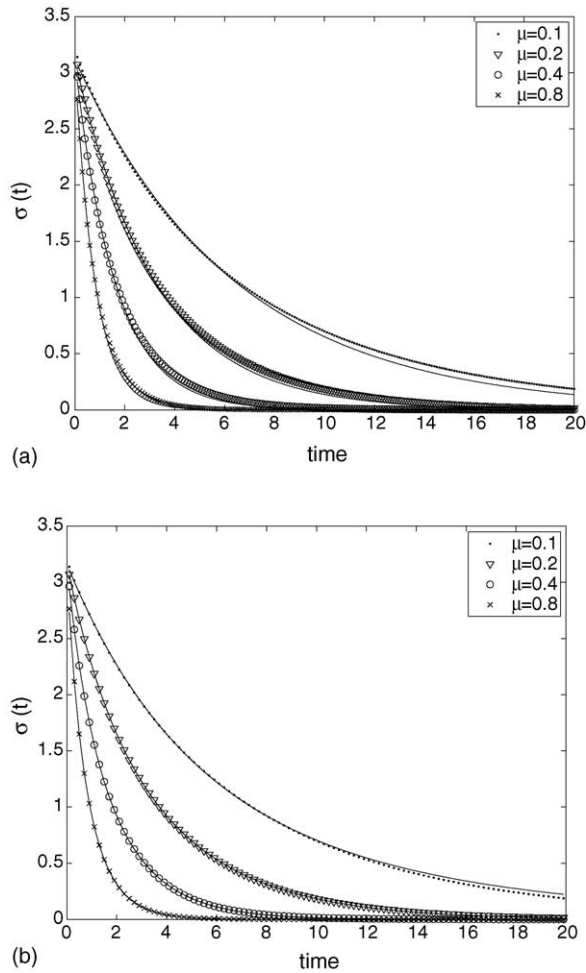


Fig. 2. The auto-covariance $\sigma(t)$ for $g(v) = \mu/(\mu^2 + v^2)$, $\beta = 1$ and various values of μ (symbols) and the exponential fits (solid lines).

Although our parameter estimation will, of course, be performed using discrete time observations of a single path of $Y_n(t)$, it is important to understand the limit in which the path is observed in continuous time. If $Y(t)$ is a continuous path on $t \in [0, T]$ then the maximum likelihood estimate (MLE) for α_0 , in a fit to Eq. (21), is [24,25]

$$\hat{\alpha}_0 = -\frac{\int_0^T Y(t) dY(t)}{\int_0^T Y^2(t) dt}. \tag{22}$$

This is found by writing the Radon–Nikodym derivative between Wiener measure and measure on path-space for the OU process. Formally the estimate may be found by a least squares calculation: set $U(t) = Y(t)$ in (21) and choose $\hat{\alpha}_0$ to minimize

$$\frac{2\alpha_0}{\beta_0} \int_0^T \left| \frac{dB}{dt} \right|^2 dt = \int_0^T \left| \frac{dY}{dt} + \alpha_0 Y \right|^2 dt$$

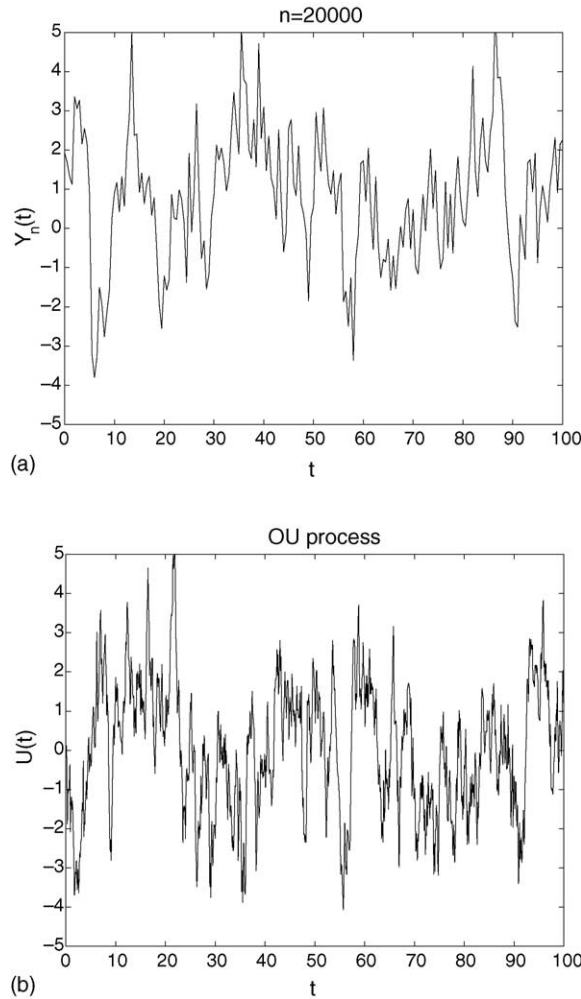


Fig. 3. (a) sample path of $Y_n(t)$ for $n = 20,000$ and $\beta = 1$. (b) sample path of the limiting OU process.

over α_0 . If $Y(t)$ is a sample path of (21) then it follows that $\hat{\alpha}_0 \rightarrow \alpha_0$ almost surely as $T \rightarrow \infty$ [25]. Once $\hat{\alpha}_0$ is estimated, the temperature β_0 can be found from the fact that, if $Y(t)$ is actually a sample path of (21), then, almost surely:

$$\sum_{i=1}^n \left[Y\left(\frac{iT}{n}\right) - Y\left(\frac{(i-1)T}{n}\right) \right]^2 \rightarrow \frac{2\alpha_0 T}{\beta_0} \tag{23}$$

as $n \rightarrow \infty$, for any fixed T .

The estimate for the drift α_0 which (22) implies can only be improved by observing the sample path on longer time intervals. For the diffusion coefficient $\alpha_0\beta_0^{-1}$, however, the estimate implied by (23) on any time interval will suffice, no matter how short; this is because diffusion is characterized by local fluctuations in the path. Since the inverse temperature β_0 requires knowledge of both drift and diffusion, it too can only be improved by sampling longer time intervals.

If the path $Y(t)$ is observed at closely spaced points in time, separated by $\Delta t \ll 1$, then we expect maximum likelihood estimation to reproduce the convergence behaviour of the continuous sample path estimates—requiring

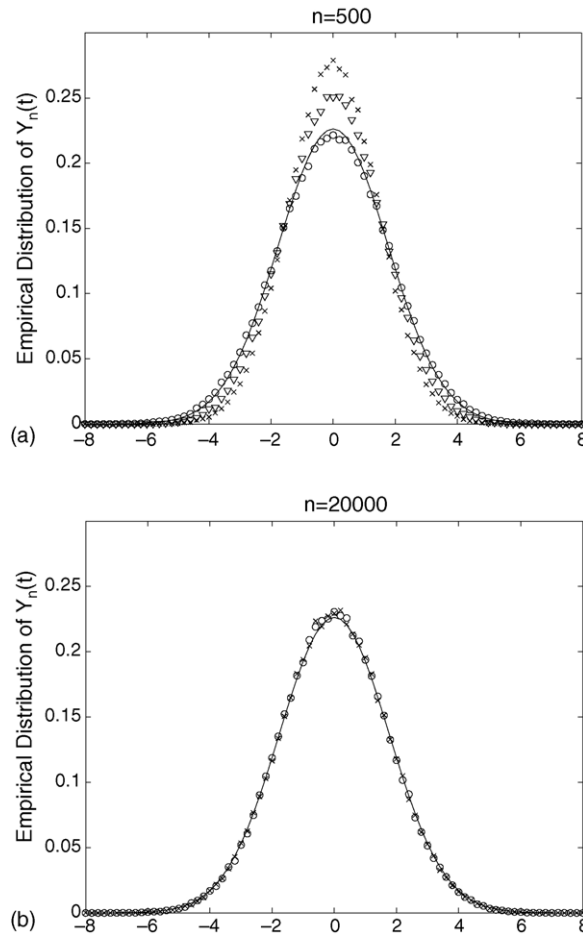


Fig. 4. Symbols: empirical distributions of sample paths of $Y_n(t)$ for $n = 500$ (a) and $n = 20,000$ (b); we used $a = 1/4$ and $\beta = 1$. Solid line: the empirical distribution of the limiting process $U(t)$.

long time intervals to estimate the drift, but not the diffusion. Now we describe how to find estimates for α_0 , β_0 in the case of discretely observed data. Let $X_j = Y(j\Delta t)$. Then, if Y is the OU process (21):

$$X_j - \lambda_0 X_{j-1} = Z_j, \quad (24)$$

where $\lambda_0 = \exp(-\alpha_0 \Delta t)$ and the Z_j are i.i.d. normal variables with mean zero and variance $\gamma_0^2 = \beta_0^{-1}[1 - \exp(-2\alpha_0 \Delta t)]$. Within the time series terminology, such a process is known as an auto-recursive process of order 1, denoted AR(1) (see e.g. [26]).

Given a sample path of X_j the parameters λ_0 , γ_0^2 (and hence α_0 , β_0) are estimated using the maximum likelihood estimation. Specifically, assuming λ_0 , γ_0^2 to be known, the one-step transition probability density from X_{j-1} to X_j , given X_{j-1} is $\mathcal{N}(\lambda_0 X_{j-1}, \gamma_0^2)$, hence the likelihood for the data $\{X_j\}$ is

$$\mathcal{L}(\lambda_0, \gamma_0^2) = \prod_{j=1}^N \frac{1}{\sqrt{2\pi\gamma_0^2}} \exp \left[-\frac{(X_j - \lambda_0 X_{j-1})^2}{2\gamma_0^2} \right].$$

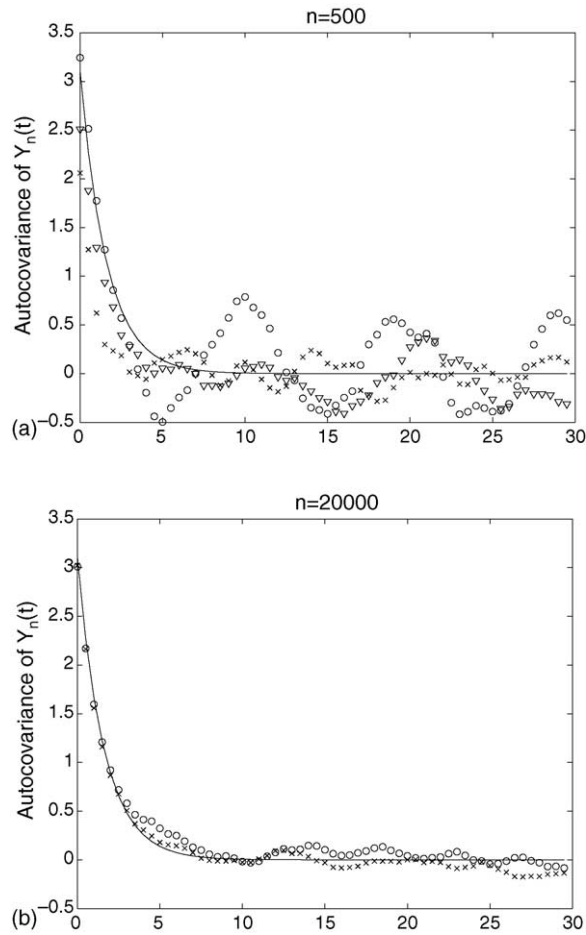


Fig. 5. Symbols: empirical auto-covariance of sample paths of $Y_n(t)$ for $n = 500$ (a) and $n = 20,000$ (b); we used $a = 1/4$ and $\beta = 1$. Solid line: the auto-covariance (19) of $U(t)$.

Maximizing the logarithm of $\mathcal{L}(\lambda_0, \gamma_0^2)$ with respect to the model parameters we obtain

$$\frac{\partial}{\partial \lambda_0} \log \mathcal{L}(\lambda_0, \gamma_0^2) = \sum_{j=1}^N \frac{X_{j-1}(X_j - \lambda_0 X_{j-1})}{\gamma_0^2} = 0,$$

$$\frac{\partial}{\partial \gamma_0^2} \log \mathcal{L}(\lambda_0, \gamma_0^2) = -\frac{N}{2\gamma_0^2} + \sum_{j=1}^N \frac{(X_j - \lambda_0 X_{j-1})^2}{2\gamma_0^4} = 0$$

from which immediately follows

$$\hat{\lambda}_0 = \frac{\sum_{j=1}^N X_{j-1} X_j}{\sum_{j=1}^N X_{j-1}^2}, \quad \hat{\gamma}_0^2 = \frac{1}{N} \sum_{j=1}^N (X_j - \lambda_0 X_{j-1})^2.$$

This, in turn, determines estimates for the parameters α_0 , β_0 of the OU process via the inverse relations

$$\hat{\alpha}_0 = -\frac{1}{\Delta t} \log \hat{\lambda}_0, \quad \hat{\beta}_0^{-1} = \frac{\hat{\gamma}_0^2}{1 - \hat{\lambda}_0^2}.$$

Note that making the approximation $\lambda_0 \approx 1 - \alpha_0 \Delta t$ and taking the limit $\Delta t \rightarrow 0$, we recover (22) and (23).

In Fig. 6 we plot estimated values of α_0 (left) and β_0^{-1} (right) for $n = 20,000$ and $\beta = 1$. To make these estimates we first generated numerical data with time-step Δt_{\min} . We then performed parameter estimation based on sampling the numerical data with time-step $\Delta t = k \Delta t_{\min}$ for various $k \in \mathbb{Z}^+$. Each estimate is repeated for several values of k and hence of the sampling time step Δt . The dashed lines are sample path estimates for a time interval of 10^5 time units; by this time convergence to the asymptotic values has been achieved and further increase in the time interval has negligible effect on the results. The open circles are ensemble averages obtained by averaging over 10^4 sets of initial data; for each set of initial data, (ξ, τ) , we computed $Y_n(t)$ and $Y_n(t + \Delta t)$, where t is a time chosen independently at random from $[0, 100]$ for each path. We then modified the estimation procedure for data by replacing averages over time by averages over the ensemble. The thick horizontal lines represent the theoretically expected values of $\alpha_0 = 0.623$ and $\beta_0^{-1} = 3.108$ predicted from the data fit to $n = \infty$ in the previous section. From these results we draw the following conclusions:

- (1) Even for n as large as 20,000 there is still significant variability between different realizations, which indicates sensitivity to the random data.
- (2) For small Δt the estimated α_0 is very different from the theoretical prediction; it is close to zero. The estimated α_0 then grows with Δt , and reaches a plateau for $\Delta t \sim 0.25$; at the plateau the value is close to the theoretical prediction. A plausible explanation is the following: for the OU approximation to be reasonable the time steps have to be large enough compared with the characteristic period of the oscillators. For $n = 20,000$ and $a = 1/4$ this characteristic period is of the order of $T/n^a \sim 0.6$.
- (3) The ensemble-averaged results are within 2% deviation from the expected parameters for $\Delta t \approx 0.25$ and larger.

In summary, the time series analysis appears to give good fits of SDE models to sums of nonlinear oscillators, provided that the sampling rate in time is not small compared with fast frequencies in the oscillators. This is a helpful platform from which to attempt SDE fits to partially observed Hamiltonian systems—and we pursue this in Section 4.

2.5. Generalization to arbitrary potentials

The weak convergence analysis in Section 2.2 uses explicitly the similarity transformation for power law valued potentials. In this section we generalize the weak convergence results for arbitrary potentials.

Consider again a single degree of freedom Hamiltonian

$$H(p, q) = \frac{p^2}{2m} + kv(q),$$

where m is the mass of the particle, $v(q)$ is the potential, and k is a spring stiffness parameter. Hamilton's equations are

$$\dot{q} = H_p(p, q) = \frac{p}{m}, \quad \dot{p} = -H_q(p, q) = -kv'(q), \quad q(0) = q_0, \quad p(0) = p_0, \quad (25)$$

where the subscripts in H_q , H_p denote differentiation. As before, the initial conditions (p_0, q_0) are drawn from the Gibbs distribution, i.e. with density $f(p_0, q_0) = (1/z) \exp[-\beta H(p_0, q_0)]$. We assume that all the trajectories $(p(t), q(t))$ solving (25) are closed.

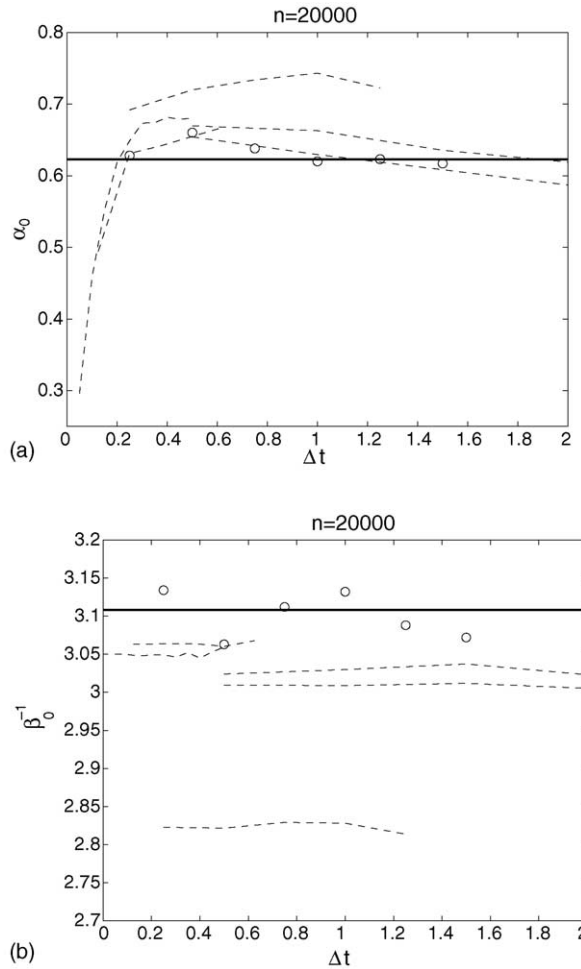


Fig. 6. Parameter fitting of Y_n to an OU process for $\beta = 1$. The dashed lines are sample path estimates over several time intervals; the open circles are ensemble average estimates. Left: estimated values of α_0 vs. Δt for different realizations. The solid line is $\alpha_0 = 0.623$, which is the value that was obtained by fitting the auto-covariance function. Right: estimated values of β_0^{-1} vs. Δt . The solid line is $\beta_0^{-1} = 3.108$.

Hamiltonian systems with one degree of freedom are integrable, implying the existence of a canonical transformation into action-angle variables [27]. Let $a(p, q)$ be the area enclosed by a trajectory $(p(t), q(t))$ of (25) that passes through the point (p, q) . Since both $H(p, q)$ and $a(p, q)$ are constant along trajectories, then there is a function $A(\cdot)$ such that

$$a(p, q) = A(H(p, q)).$$

If the level sets of $H(p, q)$ are closed and nested then this function is one-to-one and we assume that this is the case; this restriction can be partially relaxed and we will indicate what is needed for this below. The derivative $A'(H)$ has units of time; it is the period corresponding to energy H . The angular frequency is defined accordingly by

$$\nu = \frac{2\pi}{A'(H)}$$

and can be parameterized either as a function of H or a ; we will use $\nu = \nu(a)$.

The points on any given orbit can be parameterized by an “angle”, ϑ , which is time normalized so that the period in ϑ is always 2π . The origin $\vartheta = 0$ is arbitrary up to a differentiability requirement on the map $(p, q) \mapsto (a, \vartheta)$. So given (p, q) , there is an associated $a(p, q)$, the area enclosed by the orbit through (p, q) , and $\vartheta(p, q)$, which is a normalized time along that orbit. Using (a, ϑ) as coordinates in the (p, q) plane, the equations of motion are

$$\dot{a} = 0, \quad \dot{\vartheta} = v(a), \quad (26)$$

as a direct consequence of the definitions. Thus, the solution is $a(t) = a_0$ and $\vartheta(t) = v(a_0)t + \vartheta_0$. If $q(a, \vartheta)$, $p(a, \vartheta)$ denotes the inverse map, then the solution $q(t)$ to (25) is $q(t) = q(a_0, v(a_0)t + \vartheta_0)$.

Remark. For example, let $v(q) = (1/4)q^4$, then an explicit calculation yields

$$A(H) = 4 \int_0^{(4H/k)^{1/4}} \sqrt{2m \left(H - \frac{kq^4}{4} \right)} dq = \frac{4\sqrt{\pi}\Gamma(5/4)}{\Gamma(7/4)} m^{1/2} k^{-1/4} H^{3/4} \quad (27)$$

and the period is

$$T(H) = A'(H) = \frac{3\sqrt{\pi}\Gamma(5/4)}{\Gamma(7/4)} m^{1/2} k^{-1/4} H^{-1/4}.$$

The “normalized” function $\Phi(t)$ given by (7) corresponds to the parameters $k = 1$, $m = 1$ and $H = 1/4$, in which case we get a period of $T = 3\sqrt{2\pi}\Gamma(5/4)/\Gamma(7/4) = 7.4163$ as expected. Finally, we relate the action-angle variables (a, ϑ) to the variables (ξ, τ) used in Section 2.1. The phases ϑ and τ differ only by a multiplicative constant:

$$\vartheta = \frac{2\pi}{T} \tau.$$

The relation between a and ξ is deduced by noting that $H = \xi^4/4$, which together with (27) gives

$$a = \frac{\sqrt{2\pi}\Gamma(5/4)}{\Gamma(7/4)} m^{1/2} k^{-1/4} \xi^3.$$

To find the Jacobian of the mapping $(p, q) \mapsto (a, \vartheta)$ we note that

$$\dot{\vartheta} = \vartheta_q \dot{q} + \vartheta_p \dot{p} = \vartheta_q H_p - \vartheta_p H_q = v$$

and

$$a_q = A'(H)H_q = \frac{2\pi}{v} H_q, \quad a_p = A'(H)H_p = \frac{2\pi}{v} H_p,$$

so that

$$\vartheta_q H_p - \vartheta_p H_q = \frac{v}{2\pi} (\vartheta_q a_p - \vartheta_p a_q) = v.$$

Hence:

$$\left| \frac{\partial(\vartheta, a)}{\partial(q, p)} \right| = (\vartheta_q a_p - \vartheta_p a_q) = 2\pi.$$

As a consequence, the measure on (p_0, q_0) induces on (a_0, ϑ_0) a measure with density $\tilde{f}(a_0, \vartheta_0)$, where

$$\tilde{f}(a, \vartheta) = \frac{1}{2\pi} f(p(a, \vartheta), q(a, \vartheta)) = \frac{1}{Z} \exp[-\beta H(a)],$$

and $Z = 2\pi \int_0^\infty e^{-\beta H(a)} da$.

Remark. When the level sets of H are not nested, for example if $v(q)$ has multiple critical points, then there may be more than one trajectory corresponding to a given energy or action; in particular, the map $(p, q) \mapsto (a, \vartheta)$ is not one-to-one. Thus, one has to consider the possibility of $r = r(a)$ trajectories, which we denote by $q_\gamma(a, \vartheta)$, $\gamma = 1, 2, \dots, r(a)$; the corresponding energies are denoted by $H_\gamma(a)$. The measure $\tilde{f}(a, \vartheta)$ then takes the form

$$\tilde{f}(a, \vartheta) = \frac{1}{Z} \sum_{\gamma=1}^{r(a)} \exp[-\beta H_\gamma(a)],$$

where $Z = 2\pi \int_0^\infty \sum_{\gamma=1}^{r(a)} e^{-\beta H_\gamma(a)} da$. However, here we proceed on the assumption that the level sets are nested, for ease of exposition.

We now consider a collection of n oscillators, the j th oscillator having mass m_j and a spring stiffness constant k_j ; these parameters may depend on n , but we do not add an extra index to retain a compact notation. The action and angle of the j th oscillator are denoted by a_j and ϑ_j , respectively; the mapping from (a_j, ϑ_j) to the (p, q) plane is denoted by $p_j(a_j, \vartheta_j)$ and $q_j(a_j, \vartheta_j)$; the energy-action relation is $a_j = A_j(H_j)$, with $v_j = 2\pi/A'_j(H_j)$. The action variables have a probability density proportional to $\exp[-\beta H_j(a_j)]$, whereas $\vartheta_j \sim \mathcal{U}[0, 2\pi]$.

The trajectory $q_j(t)$ of the j th particle is given by $q_j(a_j, v_j(a_j)t + \vartheta_j)$, where a_j, ϑ_j are the initial action-angle values. The total force that the n oscillators exert is

$$Y_n(t) = - \sum_{j=1}^n m_j v_j^2(a_j) \frac{\partial^2 q_j}{\partial \vartheta_j^2}(a_j, v_j t + \vartheta_j) = \sum_{j=1}^n k_j v'(q_j(a_j, v_j t + \vartheta_j)). \tag{28}$$

Note that, if \mathbb{E} denotes expectation with respect to random data on (a, ϑ) :

$$\begin{aligned} \mathbb{E} \left[v_j^2 \frac{\partial^2 q_j}{\partial \vartheta_j^2}(a_j, v_j t + \vartheta_j) \right] &= \frac{1}{Z_j} \int_0^\infty v_j^2 e^{-\beta H_j} \int_0^{2\pi} \frac{\partial^2 q_j}{\partial \vartheta_j^2}(a_j, v_j t + \vartheta_j) d\vartheta_j da_j \\ &= \frac{1}{Z_j} \int_0^\infty v_j^2 e^{-\beta H_j} \left[\frac{\partial q_j}{\partial \vartheta_j}(a_j, v_j t + 2\pi) - \frac{\partial q_j}{\partial \vartheta_j}(a_j, v_j t) \right] da_j = 0, \end{aligned} \tag{29}$$

where the last equality follows from the periodicity in ϑ of $q(a, \vartheta)$; here

$$Z_j = 2\pi \int_0^\infty \exp[-\beta H_j(a)] da.$$

Thus $\mathbb{E}Y_n(t) = 0$. The auto-covariance, $\sigma_n(t) = \mathbb{E}Y_n(s)Y_n(s+t)$, is given by

$$\sigma_n(t) = \sum_{j=1}^n \frac{k_j^2}{Z_j} h_j(v_j t), \quad h_j(t) = \int_0^\infty e^{-\beta H_j} \int_0^{2\pi} v'(q_j(a_j, t + \vartheta_j))v'(q_j(a_j, \vartheta_j)) d\vartheta_j da_j. \tag{30}$$

Note that the structure is very similar to that in [Section 2.2](#). Analogously to the conditions leading to the proof of [Theorem 2.1](#) we anticipate that, under certain assumptions on the behaviour of the masses m_j and spring constants

k_j (and hence on H_j , A_j and v_j), the function $\sigma_n(t)$ will have a limit as $n \rightarrow \infty$ and that this will characterize a limiting mean-zero stationary Gaussian process $Y(t)$ found from $Y_n(t)$ in the limit as $n \rightarrow \infty$. Rigorous analysis of this situation will not be undertaken here; it is similar to, but more involved than, that for the proof of [Theorem 2.1](#).

3. Drag force on a moving body coupled to nonlinear oscillators

In this section we generalize our insights from [Section 2](#) to the situation where the nonlinear oscillators have a moving anchor point, $Q(t)$. This is in preparation for [Section 4](#) where $Q(t)$ will itself couple back to the oscillators through a Hamiltonian; the situation in [Section 4](#) is, of course, the primary goal of our studies.

In this section we show that, given a function $Q(t)$, the effective force may be split into a “drag” (zero if $Q(t) = 0$ as in the previous section) and “fluctuations” (the object of study in the previous section). We use approximations which assume that $Q(t)$ is small. In practice we find their range of validity to be surprisingly large.

In [Section 3.1](#) we consider a single nonlinear oscillator; in [Section 3.2](#) we extend the validity of our analysis by means of numerical experiment. In [Section 3.3](#) we study a collection of oscillators with differing masses and spring constants.

3.1. A moving body coupled to a single oscillator

Consider again a single nonlinear oscillator of mass m and spring potential $kv(q)$. This time the oscillator’s anchor point moves; we denote its trajectory by $Q(t)$. We may regard the motion of the oscillator as governed by a time dependent Hamiltonian:

$$H(p, q, t) = \frac{p^2}{2m} + kv(q - Q(t)).$$

Hamilton’s equations are

$$\dot{q} = \frac{p}{m}, \quad \dot{p} = -kv'(q - Q(t))$$

with initial data (p_0, q_0) distributed with density $(1/z) \exp[-\beta H(p_0, q_0, 0)]$ (a Gibbs distribution *conditioned by the initial data for $Q(t)$*). Note that this distribution is not invariant when $Q(t)$ is not constant in time.

The quantity of interest is the force $F(t)$ exerted by the oscillator:

$$F(t) = kv'(q(t) - Q(t)), \tag{31}$$

which we write as the sum of two terms: the expected value, $\bar{F}(t) = \mathbb{E}F(t)$, which we call the “drag”, and the deviation from the mean, $\tilde{F}(t) = F(t) - \bar{F}(t)$, which we call “fluctuations”. As usual \mathbb{E} denotes expectation with respect to random initial data.

It is more convenient to use a centered coordinate, $q(t) \mapsto q(t) + Q(t)$, in terms of which

$$\dot{q} = \frac{p}{m} - \dot{Q}, \quad \dot{p} = -kv'(q). \tag{32}$$

Eqs. (32) are Hamilton’s equations for a time-dependent Hamiltonian

$$H_1(p, q, t) = \frac{p^2}{2m} + kv(q) - p\dot{Q}(t) \equiv H(p, q) - p\dot{Q}(t).$$

The force is now

$$F(t) = kv'(q(t)). \tag{33}$$

The initial data (p_0, q_0) are distributed with density $f(p_0, q_0)$, where

$$f(p, q) = \frac{1}{Z} \exp \left[-\beta \left(\frac{p^2}{2m} + kv(q) \right) \right]. \tag{34}$$

As in the static (or unperturbed) case we use action-angle variables. Let (a, ϑ) be action-angle variables *as constructed with the unperturbed Hamiltonian*, $H(p, q)$. The equations of motion for (a, ϑ) are

$$\dot{a} = a_q \dot{q} + a_p \dot{p} = a_q(H_p - \dot{Q}) - a_p H_q, \quad \dot{\vartheta} = \vartheta_q \dot{q} + \vartheta_p \dot{p} = \vartheta_q(H_p - \dot{Q}) - \vartheta_p H_q.$$

Because $H_q = (\nu/2\pi)a_q$, $H_p = (\nu/2\pi)a_p$, and $\vartheta_q a_p - \vartheta_p a_q = 2\pi$, we obtain

$$\dot{a} = -a_q \dot{Q}, \quad \dot{\vartheta} = \nu(a) - \vartheta_q \dot{Q}. \tag{35}$$

Indeed, if $\dot{Q}(t) \equiv 0$ then (35) reduces to the trivial unperturbed system (26). To transform the right hand sides into functions of (a, ϑ) only we use the following identity:

$$\begin{pmatrix} \vartheta_q & \vartheta_p \\ a_q & a_p \end{pmatrix} = \begin{pmatrix} q_\vartheta & q_a \\ p_\vartheta & p_a \end{pmatrix}^{-1} = 2\pi \begin{pmatrix} p_a & -q_a \\ -p_\vartheta & q_\vartheta \end{pmatrix},$$

so that $a_q = -2\pi p_\vartheta$, $\vartheta_q = 2\pi p_a$, and

$$\dot{a} = 2\pi p_\vartheta(a, \vartheta) \dot{Q}, \quad \dot{\vartheta} = \nu(a) - 2\pi p_a(a, \vartheta) \dot{Q}. \tag{36}$$

Recall that $\nu(a) = 2\pi H'(a)$, hence (36) is a Hamiltonian system with time-dependent Hamiltonian

$$G(a, \vartheta, t) = 2\pi [H(a) - \dot{Q}(t)p(a, \vartheta)].$$

The initial data are distributed with density

$$\tilde{f}(a) = \frac{1}{Z} \exp[-\beta H(a)],$$

where $Z = 2\pi \int_0^\infty e^{-\beta H(a)} da$.

Eq. (36) cannot be solved analytically. However, since we are only interested in the evolving statistics of an ensemble of solutions, we may consider instead the effect that the perturbation by Q has on the probability density, $\rho(a, \vartheta, t)$, in the action-angle plane. This density satisfies the Liouville equation

$$\frac{\partial \rho}{\partial t} = -\frac{\partial}{\partial a} (2\pi p_\vartheta \dot{Q} \rho) - \frac{\partial}{\partial \vartheta} [(\nu(a) - 2\pi p_a \dot{Q}) \rho] = -2\pi p_\vartheta \dot{Q} \frac{\partial \rho}{\partial a} - (\nu(a) - 2\pi p_a \dot{Q}) \frac{\partial \rho}{\partial \vartheta} \tag{37}$$

with initial density

$$\rho(a, \vartheta, 0) = \tilde{f}(a).$$

For future use, note that

$$\frac{\partial}{\partial a} \tilde{f}(a) = -\beta H'(a) \tilde{f}(a) = -\frac{\beta}{2\pi} v(a) \tilde{f}(a).$$

In the unperturbed case, $\dot{Q}(t) \equiv 0$, the solution is stationary, $\rho(a, \vartheta, t) = \tilde{f}(a)$. For weak perturbations we expect the density to deviate from $\tilde{f}(a)$ only slightly. To carry out a formal power series expansion we set $\dot{Q}(t) \mapsto \epsilon \dot{Q}(t)$ (ϵ is eventually set to 1), and expand the density in powers of ϵ :

$$\rho(a, \vartheta, t) = \tilde{f}(a) + \epsilon \rho_1(a, \vartheta, t) + \epsilon^2 \rho_2(a, \vartheta, t) + \dots$$

Substituting this expansion into the Liouville equation (37), equating terms of the same order in ϵ , we obtain for the $O(\epsilon)$ terms:

$$\frac{\partial \rho_1}{\partial t} + v(a) \frac{\partial \rho_1}{\partial \vartheta} = -2\pi p_\vartheta(a, \vartheta) \dot{Q}(t) \frac{\partial \tilde{f}}{\partial a} = \beta v(a) p_\vartheta(a, \vartheta) \dot{Q}(t) \tilde{f}(a) = -\beta k v'(q(a, \vartheta)) \dot{Q}(t) \tilde{f}(a). \quad (38)$$

In the last identity we used the fact that p_ϑ is the time derivative of the momentum, where time is measured in units of $1/v$, hence $v p_\vartheta$ is the force exerted by the oscillator, $k v'(q)$.

The homogeneous part of the linear equation (38) governs translation along the angular coordinate. Thus, the solution to the inhomogeneous equations is given by Duhamel's principle:

$$\rho_1(a, \vartheta, t) = -\beta k \tilde{f}(a) \int_0^t v'(q(a, \vartheta - v(a)(t-s))) \dot{Q}(s) ds,$$

where we have imposed the initial perturbation $\rho_1(a, \vartheta, 0) = 0$.

The force exerted by an oscillator with coordinates (a, ϑ) is $k v'(q(a, \vartheta))$. Therefore, over a distribution of initial conditions, the mean force is

$$\bar{F}(t) = k \int_0^\infty \int_0^{2\pi} v'(q(a, \vartheta)) \rho(a, \vartheta, t) d\vartheta da.$$

We substitute the first order approximation for $\rho(a, \vartheta, t)$. The zeroth order term vanishes (there is no drag in the absence of perturbations—see Eq. (29)—and so, to leading order and setting $\epsilon = 1$, we obtain

$$\bar{F}(t) \approx - \int_0^t \kappa(t-s) \dot{Q}(s) ds, \quad (39)$$

where

$$\kappa(t) = \beta k^2 \int_0^\infty \int_0^{2\pi} v'(q(a, \vartheta - v(a)t)) v'(q(a, \vartheta)) \tilde{f}(a) d\vartheta da. \quad (40)$$

Eq. (39) is a linear response solution (see Chapter 5 in [28] for general reference on linear response theory). The drag depends linearly on the perturbation. This dependence is non-local in time, and involves a convolution with a memory kernel, $\kappa(t)$. Furthermore, since $\tilde{f}(a)$ is the canonical density for the oscillator, the memory kernel (40) multiplied by the temperature $1/\beta$ coincides with the auto-covariance of the fluctuating force $\bar{F}(t)$ at equilibrium, i.e., when $\dot{Q}(t) \equiv 0$. This is a manifestation of the fluctuation–dissipation principle. Note, however, that linear response is a consequence of our weak perturbation asymptotics. It is not expected to remain valid for arbitrarily large perturbations.

3.2. Numerical results

In the previous section we considered the drag (i.e., mean) force that a single oscillator with Gibbsian initial data exerts on its anchor point when the latter moves. We were able to derive an explicit expression in a near equilibrium regime. We now verify numerically the accuracy of the linear response approximation.

Given $Q(t)$ the drag force $\bar{F}(t)$ can be calculated numerically as follows. A set of initial data (p_0, q_0) is drawn from the distribution (34). For every initial state we integrate (32) numerically, using a standard ODE solver, and compute $F(t)$ given by (33). The mean force $\bar{F}(t)$ is estimated by averaging over the ensemble. We used a sample of 5000 solutions, which proved sufficient to get small enough sampling errors.

Plots of the mean force are shown in Figs. 7–10 and comparisons are made with the linear response prediction (39). All our calculations are for the quartic potential $v(q) = (1/4)q^4$ with $m = k = 1$. As discussed above, the memory kernel $\kappa(t)$ equals β times the auto-covariance (16) of the force exerted by a single oscillator at equilibrium. In Fig. 7 we show the drag for the case where the anchor point is translated with constant speed, $Q(t) = \gamma t$, and $\beta = 1$ (solid lines). We repeat this calculation for four values of γ , and compare the computed curves with the linear response solution (dashed curves), which in this case takes the simple form

$$\bar{F}(t) \approx -\gamma \int_0^t \kappa(t-s) ds = -\gamma\beta \int_0^t \beta^{-3/2} h(\beta^{-1/4}(t-s)) ds = -\gamma\beta^{-1/4} \int_0^{\beta^{-1/4}t} h(s) ds. \tag{41}$$

Both the exact and the approximate solution exhibit decaying oscillations. The linear response solution fits the exact solution very well when the translation rate is $\gamma = 0.5$, and is even fairly good for $\gamma = 1$. But its accuracy deteriorates as γ increases further and nonlinear effects become significant. Note that in the nonlinear regime the amplitude of the drag grows nonlinearly with γ , and the frequency of the oscillations increases with the amplitude, which is a manifestation of the amplitude dependent frequency of the oscillator.

Similar calculations are repeated in Fig. 8, this time for an abrupt perturbation, $Q(t) = \gamma H(t)$, where $H(t)$ is the Heaviside step function. Again, using (16), the linear response approximation is

$$\bar{F}(t) \approx -\gamma \int_0^t \kappa(t-s) H'(s) ds = -\gamma\kappa(t) = -\gamma\beta^{-1/4} h(\beta^{-1/4}t). \tag{42}$$

Here too, the approximation is very good when the perturbation is sufficiently weak. For stronger perturbations, the nonlinearity has a similar effect as in the case of constant translation rate.

Similar results are displayed in Figs. 9 and 10 for a higher temperature, $1/\beta = 4$. These results show that the linear response approximation is more accurate at higher temperature. This is presumably because the anchor point $Q(t)$ typically undergoes small motions, relative to the bath, as the temperature increases.

3.3. A moving body coupled to n nonlinear oscillators

Consider now a collection of n independent nonlinear oscillators attached to a common moving anchor point, whose trajectory is $Q(t)$. We allow the Hamiltonians of the oscillators to vary, as in Section 3, by making the masses m_j and coupling constants k_j into variables. All parameterizations remain the same as in Section 2.5. The goal is to characterize the force exerted by the n oscillators.

Recall that we write the total force exerted on the anchor point as

$$F_n(t) = \bar{F}_n(t) + \tilde{F}_n(t),$$

where $\bar{F}_n = \mathbb{E}F_n(t)$. By writing the anchor point trajectory as $\epsilon Q(t)$, expanding in powers of ϵ and extending the analysis of Section 3.1 to sum over variable m_j and k_j we deduce that $\bar{F}_n(t)$ is given by

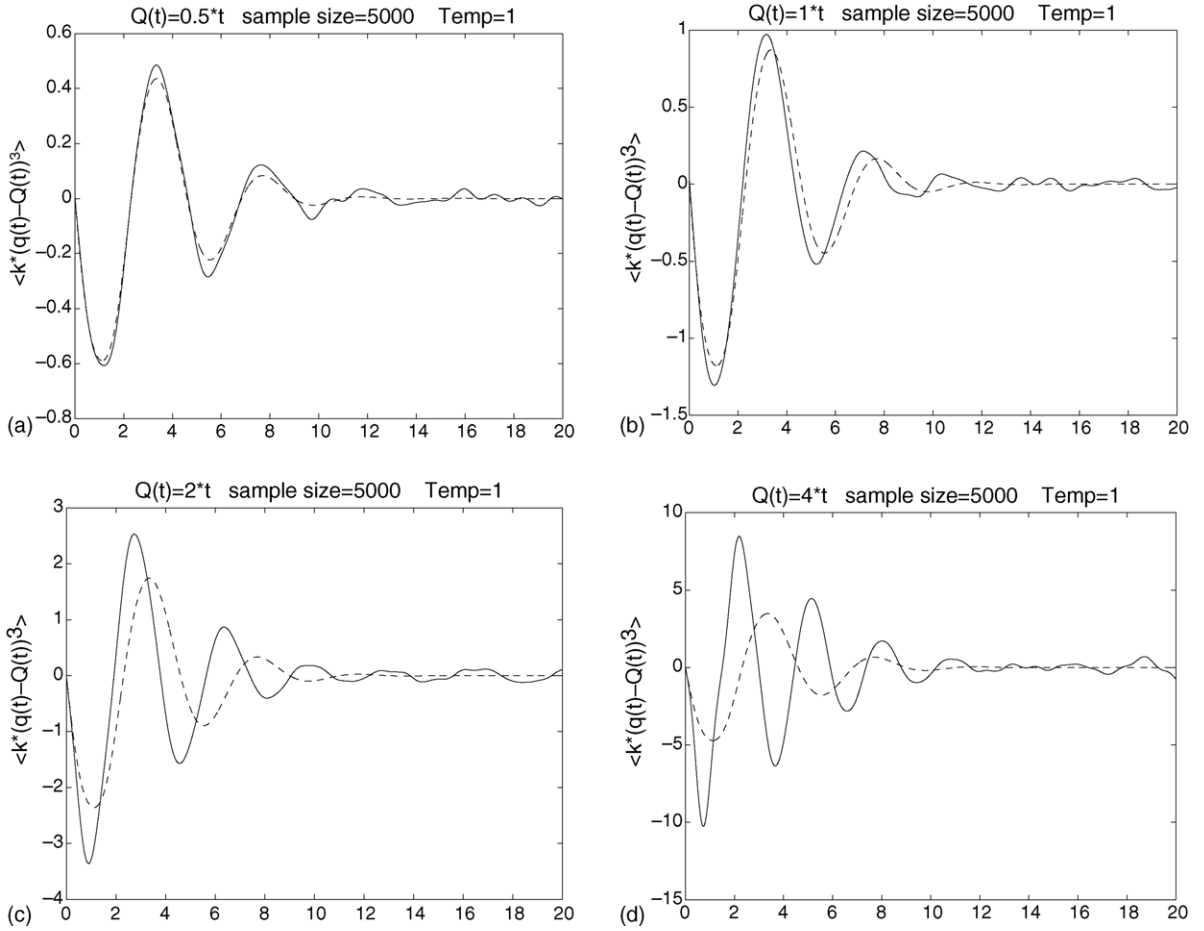


Fig. 7. Solid lines: the drag force $\bar{F}(t)$ for a steadily moving anchor point, $Q(t) = \gamma t$. These curves were computed by averaging over an ensemble of 5000 solutions. Dashed lines: the linear response prediction (41). The four plots correspond to pulling rates of $\gamma = 0.5, 1, 2,$ and 4 . The temperature is $1/\beta = 1$.

$$\bar{F}_n(t) = -\epsilon \int_0^t \mathcal{K}_n(t-s) \dot{Q}(s) ds + \mathcal{O}(\epsilon^2). \quad (43)$$

Here

$$\mathcal{K}_n(t) = \beta \sigma_n(t) \quad (44)$$

with $\sigma_n(t)$ given by (30). By the discussion in Section 2.5 (and by Theorem 2.1 for quartic coupling potentials) we expect that, under certain reasonable conditions:

$$\lim_{n \rightarrow \infty} \mathcal{K}_n(t) = \beta \sigma(t),$$

where $\sigma(t)$ is the limiting auto-covariance in the unperturbed case. On the other hand, the work of Section 2 for $\epsilon = 0$ shows that

$$\tilde{F}_n(t) = Y_n(t) + \mathcal{O}(\epsilon), \quad (45)$$

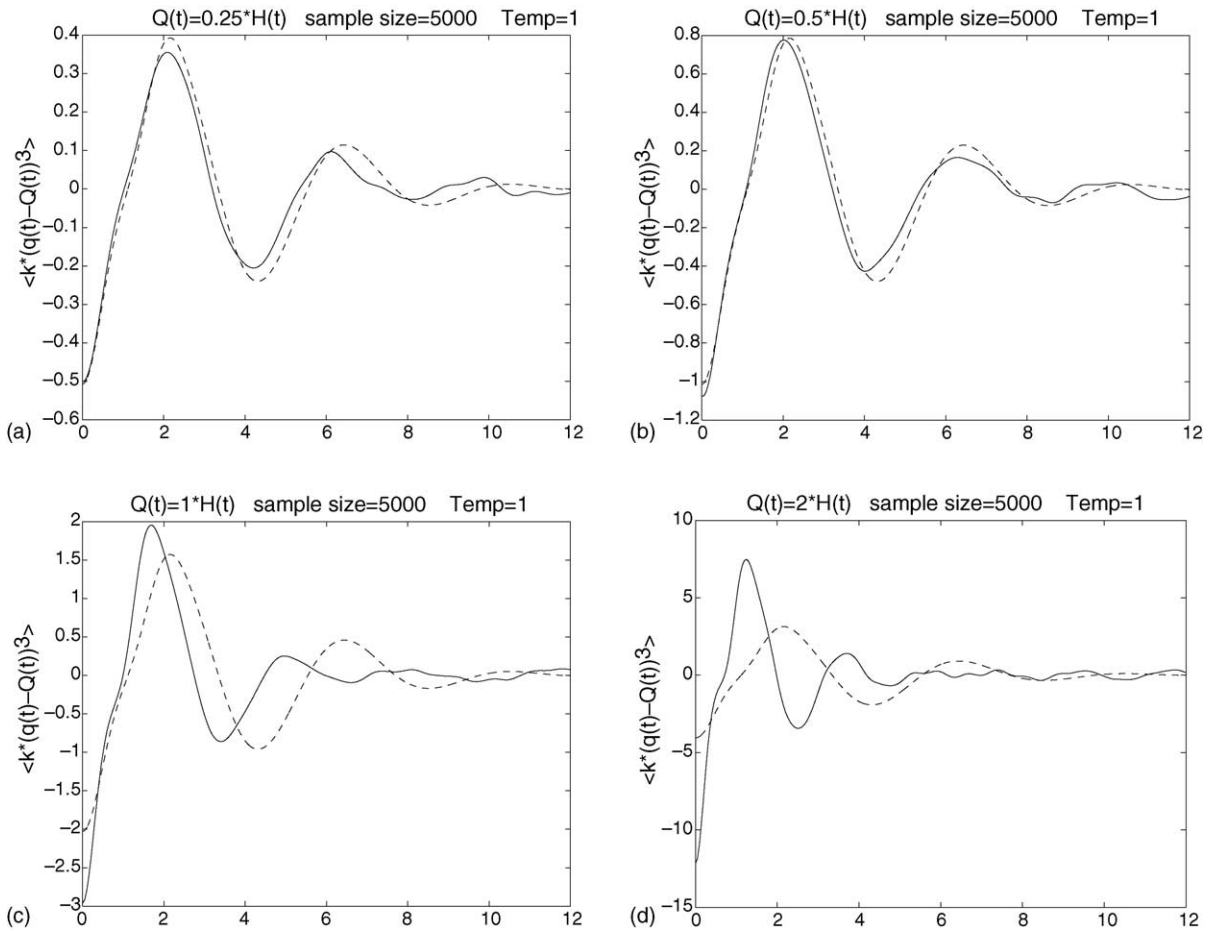


Fig. 8. Solid lines: the drag force $\bar{F}(t)$ when the anchor point jumps discontinuously at time $t = 0$: $Q(t) = \gamma H(t)$ (H is the Heaviside step function). These curves were computed by averaging over an ensemble of 5000 solutions. Dashed lines: the linear response prediction (42). The four plots correspond to $\gamma = 0.25, 0.5, 1,$ and 2 . The temperature is $1/\beta = 1$.

where $Y_n(t)$ is a stationary Gaussian process with correlation function

$$\mathbb{E}Y_n(t)Y_n(0) = \beta^{-1}\mathcal{K}_n(t) = \sigma_n(t). \tag{46}$$

Retaining only the leading order expressions in (43) and (45), and then setting $\epsilon = 1$, gives the following approximation to the force exerted on the anchor point:

$$F_n(t) = - \int_0^t \mathcal{K}_n(t-s)\dot{Q}(s) ds + Y_n(t).$$

Taking the limit $n \rightarrow \infty$ gives the force

$$F(t) = - \int_0^t \mathcal{K}(t-s)\dot{Q}(s) ds + Y(t),$$

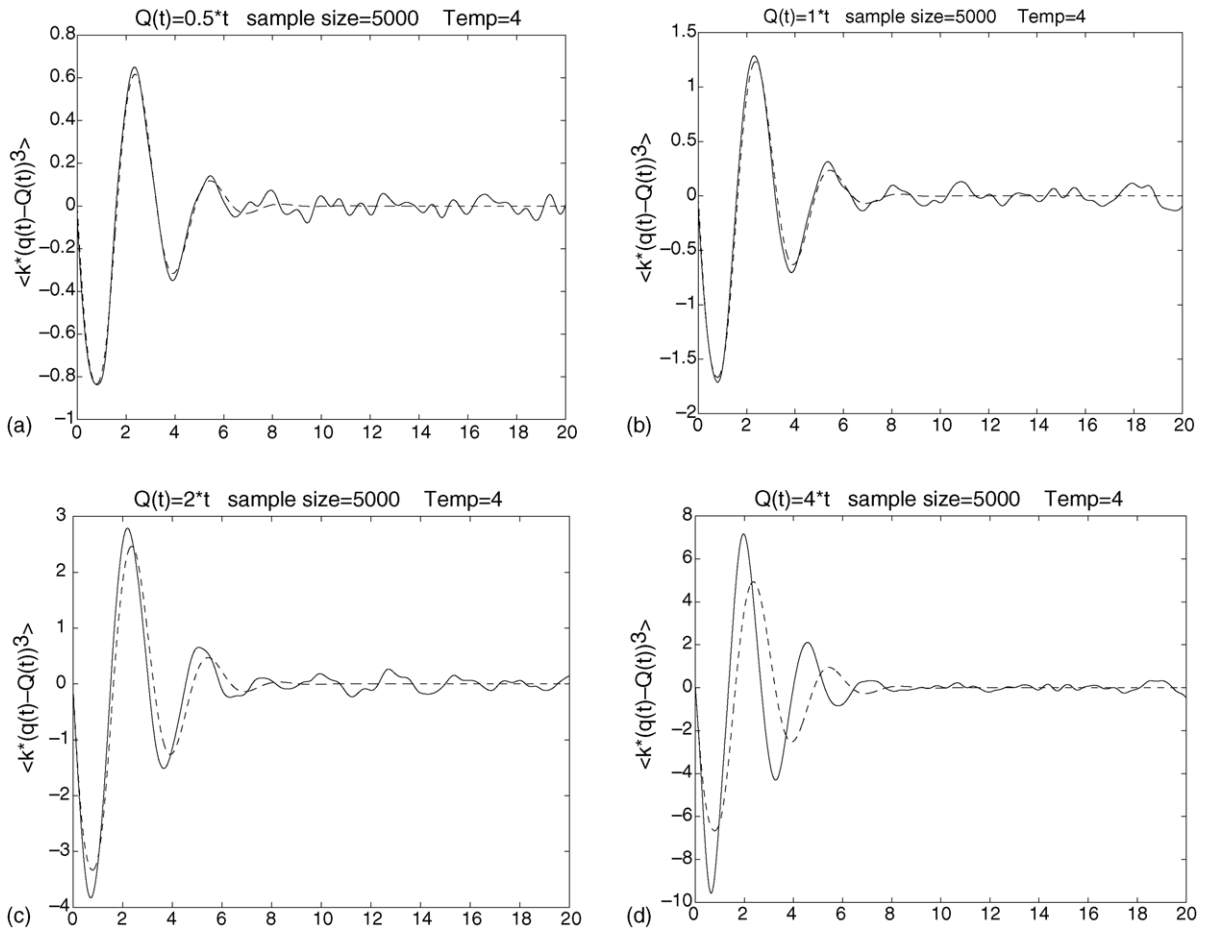


Fig. 9. Same as Fig. 7 with temperature $1/\beta = 4$.

where $Y(t)$ is a Gaussian process satisfying

$$\mathbb{E}Y(t)Y(0) = \beta^{-1}\mathcal{K}(t) = \sigma(t). \quad (47)$$

Performing an expansion of the drag and the fluctuation in $\epsilon \ll 1$, retaining only leading order terms in each expansion separately, adding them to find the effective force and then setting $\epsilon = 1$, is clearly a highly questionable procedure. However we will show in the next section that it is an approximation process which leads to quite accurate approximation of components of large Hamiltonian systems by SDEs, even in situations where $Q(t)$ is not obviously small. Note also that the idea that fluctuation and dissipation can contribute at different order in nonlinearly coupled bath-particle systems is something that has been observed in previous work—see [16] and the references therein.

4. The Hamiltonian system

In this section we put together the experience gained in previous sections in order to study the Hamiltonian heat bath models which are our primary motivation in this paper. In Section 4.1 we show how the analysis of the previous two sections leads naturally to conjectured forms for SDEs approximating the motion of a distinguished

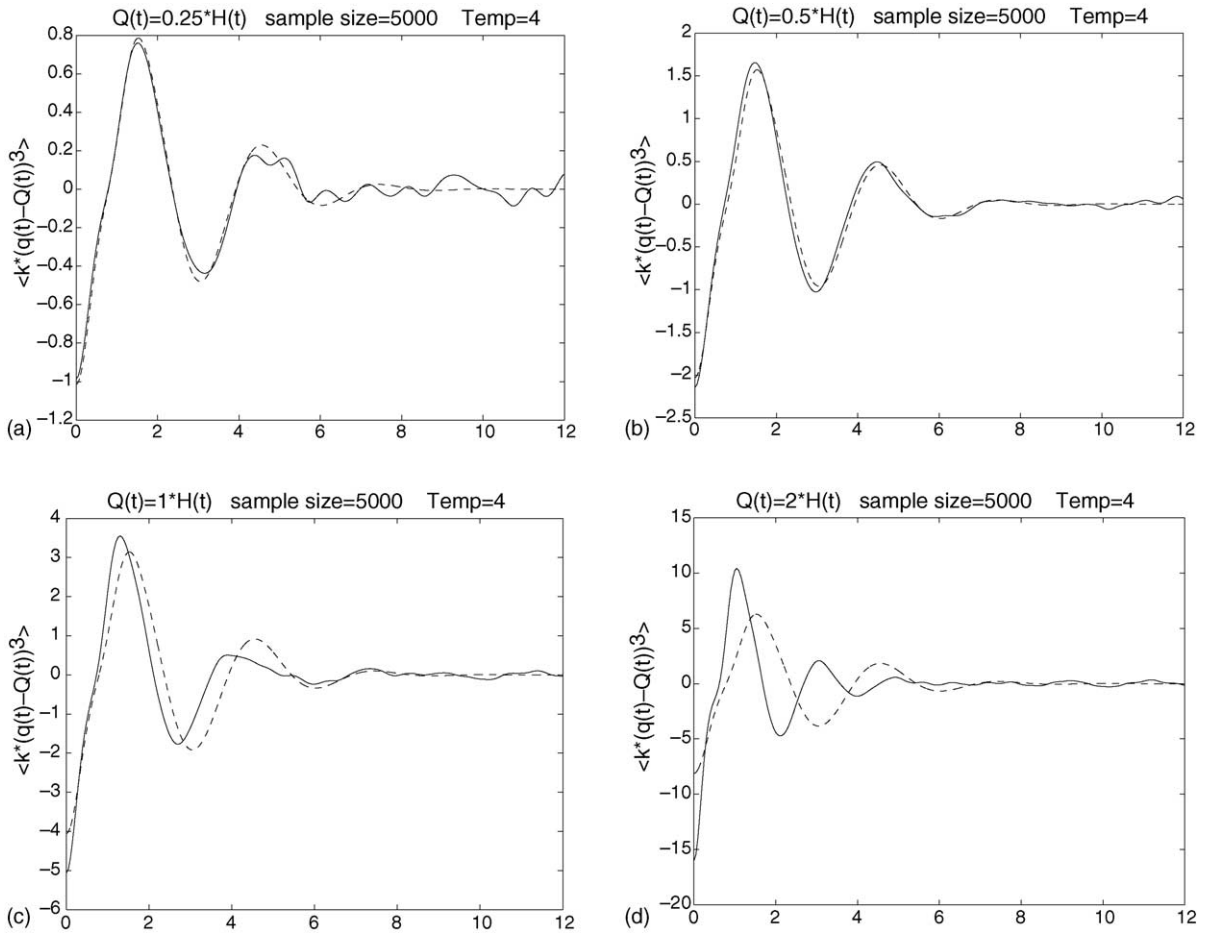


Fig. 10. Same as Fig. 8 with temperature $1/\beta = 4$.

particle coupled to a heat bath. Then, in Section 4.2, we use parameter fits obtained in Section 2.3 to determine coefficients in these SDE models and compare the behaviour of the resulting SDEs with behaviour of the underlying Hamiltonian problem. Finally, in Section 4.3, we fit the SDE models directly to data generated by sample paths of the Hamiltonian system, using time series analysis, and compare results with those from the preceding section.

4.1. The model

In the two previous sections we developed the tools necessary for the study of nonlinear heat bath models. We consider now a mechanical system that consists of $n + 1$ particles: a “distinguished” particle, whose momentum and coordinate we denote by (P_n, Q_n) , and n “heat bath” particles whose momenta and coordinates we denote by (p_j, q_j) , $j = 1, 2, \dots, n$. (The subscript n in (P_n, Q_n) is introduced purely to label the size of the heat bath.) The distinguished particle has unit mass whereas the j th heat bath particle has mass m_j . The distinguished particle moves in a potential field $V(Q_n)$, and in addition interacts with each of the n heat bath particles through a potential $k_j v(q_j - Q_n)$, where k_j is, as before, the stiffness constant of the j th interaction.

The Hamiltonian of the system is given by (1) and Hamilton's equations are:

$$\dot{Q}_n = P_n, \quad \dot{P}_n = -V'(Q_n) + \sum_{j=1}^n k_j v'(q_j - Q_n), \quad \dot{q}_j = \frac{p_j}{m_j}, \quad \dot{p}_j = -k_j v'(q_j - Q_n). \quad (48)$$

Let P_0, Q_0 denote the initial data for the distinguished particle; they are assumed to be deterministic. The heat bath variables, on the other hand, are assumed to have random initial data, $p_j(0) = p_j^0$ and $q_j(0) = q_j^0$, whose probability density is governed by the (conditional) Gibbs distribution $f(p^0, q^0)$, where $p^0 = (p_1^0, \dots, p_n^0)^T$, $q^0 = (q_1^0, \dots, q_n^0)^T$, and

$$f(p, q) = \frac{1}{Z} \exp[-\beta H(P_0, Q_0, p, q)].$$

Note that the initial data $p_1^0, \dots, p_n^0, q_1^0, \dots, q_n^0$ are mutually independent variables, by virtue of the structure in (1). Although the initial data is random, all the parameter estimation that we perform in this section is based on a single path of the underlying dynamics, generated by a single pick of the initial data.

In the case of linear springs, that is, $v(q) = (1/2)q^2$, each of the (p_j, q_j) equations in (48) can be solved explicitly, with $Q_n(t)$ as a time-dependent inhomogeneous term. Substituting the solution back into the equation for $P_n(t)$, one gets a closed integro-differential system for (P_n, Q_n) . This procedure cannot be carried out in explicit form when the interactions are nonlinear. However, the analysis of Section 3.3 suggests how to approximate the force exerted by the bath on the distinguished particle. Specifically it suggests that

$$\sum_{j=1}^n k_j v'(q_j - Q_n) \approx - \int_0^t \mathcal{K}_n(t-s) \dot{Q}_n(s) ds + Y_n(t),$$

where Y_n and \mathcal{K}_n are given by (44) and (46). This is precisely the form *proven* to be a valid approximation when there is a linear bath-particle coupling [10].

This suggests that the equation satisfied by $Q_n(t)$ is approximated by the integro-differential equation:

$$\ddot{Q}_n + V'(Q_n) + \int_0^t \mathcal{K}_n(t-s) \dot{Q}_n(s) ds = Y_n(t).$$

In the case of the quartic coupling potential as studied in Section 2.2 we know that, as $n \rightarrow \infty$, \mathcal{K} uniformly converges, on bounded intervals, to $\beta\sigma(t)$, where $\sigma(t)$ is the limiting auto-covariance. Furthermore, $Y_n(t)$ converges weakly to a stationary Gaussian processes, $Y(t)$, with mean zero and auto-covariance $\sigma(t)$. Under appropriate conditions on the distribution of masses and spring constants we expect similar convergence for general coupling potentials as well—see Section 2.5. We assume that we are operating under such conditions.

The strong convergence of the memory kernel, $\mathcal{K}_n \rightarrow \mathcal{K}$, with the weak convergence of the random forcing, $Y_n \Rightarrow Y$, imply the weak convergence of the trajectories Q_n to a limiting process Q . Specifically, $Q_n \Rightarrow Q$ in $C^2[0, T_0]$, where $Q(t)$ satisfies the stochastic integro-differential equation (SIDE):

$$\ddot{Q} + V'(Q) + \int_0^t \mathcal{K}(t-s) \dot{Q}(s) ds = Y(t) \quad (49)$$

(see [10]).

Consider again the particular case of a quartic potential $v(q) = (1/4)q^4$, with k_j governed by Assumption 2.1 and $g(v)$ given by (18), so that $\sigma(t)$ (and hence $\mathcal{K}(t)$) is well approximated by an exponential function (19). Then, using this exponential approximation and introducing an auxiliary variable $R(t)$, the SIDE (49) is approximated by

the memoryless SDE:

$$dQ = P dt, \quad Q(0) = Q_0, \quad dP = [-V'(Q) + R] dt, \quad P(0) = P_0, \quad (50)$$

$$dR = -(\alpha_0 R + \beta \beta_0^{-1} P) dt + (2\alpha_0 \beta_0^{-1})^{1/2} dB, \quad R(0) = \mathcal{N}(0, \beta_0^{-1}). \quad (51)$$

Note that

$$R(t) = -\frac{\beta}{\beta_0} \int_0^t e^{-\alpha_0(t-s)} P(s) ds + U(t),$$

where $U(t)$ is the OU process (21) with auto-covariance $\sigma(t) = \beta_0^{-1} \exp(-\alpha_0 t)$. We write the parametric dependence of the SDE for R in the form given in order to facilitate direct comparison with the SDE (21) and the parameter fits to α_0, β_0 which we obtained in Section 2.

We introduce the three free parameters α_0, β_0 and β in this fashion because, when using our analysis from $n = \infty$ to make informed choices of the parameters, this is the natural way to write the problem.

Comment: The SIDE (49) can be approximated by a memoryless SDE through the addition of auxiliary variables even when the memory kernel is not exponential. This approach holds, for example, in the extreme non-Markovian case where the memory kernel decays algebraically and the corresponding noise is a “ $1/f$ -noise”; see [29] and references therein.

4.2. Comparison of Hamiltonian system and SDE

In this section we compare statistical properties of the Hamiltonian system (48) with the SDE (50). The parameters α_0, β_0 are chosen, given β , according to the relations (20); thus we are using our linear response analysis of the previous section to inform our choice of matching SDE. In the next section we will, instead, use time series analysis directly on paths of the Hamiltonian systems to fit parameters; we will compare the resulting parameter estimates.

In Fig. 11 we plot a sample path of $Q_n(t)$ solving the Hamiltonian system, with $n = 2500, \beta = 1$, and a double-well self-potential $V(Q) = (1/4)Q^4 - (1/2)Q^2$. For comparison, we also plot a sample path of $Q(t)$ solving the approximating SDE. In both cases, the distinguished particle spends most of its time in the vicinity of the wells’ minima, $Q = \pm 1$, with occasional jumps between wells. We now quantify the similarity between the two systems.

In Fig. 12 we plot the empirical distributions (left) and the empirical auto-covariances (right) for four sample paths of $Q_n(t)$ solving the Hamiltonian system (48) with a quadratic self-potential, $V(Q) = (1/2)Q^2$ and temperature $\beta^{-1} = 1$; as before we take $a = 1/4$. These results are represented by dashed lines; the solid lines are the same quantities for a sample path of $Q(t)$ solving the SDE (50). The top graphs are for $n = 1000$ and the bottom ones for $n = 2500$. For $n = 1000$ there is still significant variability between different realizations. This variability is much smaller for $n = 2500$, and the data agrees quite well with the data for the SDE, indicating that the linear response approximation works well.

Similar data are presented in Fig 13, this time for a double-well shaped self-potential, $V(Q) = (1/4)Q^4 - (1/2)Q^2$. Here again, there is a significant reduction in variance when the number of particles increases from 1000 to 2500. The agreement between the larger system and the approximating SDE is excellent for $n = 2500$.

Finally, in Fig. 14 we repeat the double-well calculations for a higher temperature, $1/\beta = 4$. Consistent with the results in the previous section, higher temperature improves the quality of the linear response approximation and there is even better agreement between statistical properties of the Hamiltonian system and the approximating SDE. In fact it appears that the errors are dominated by sampling for the $n = 2500$ case.

In conclusion, we have shown that linear response theory predicts an SDE fit to the partially observed Hamiltonian which is very good for moderate to high temperatures.

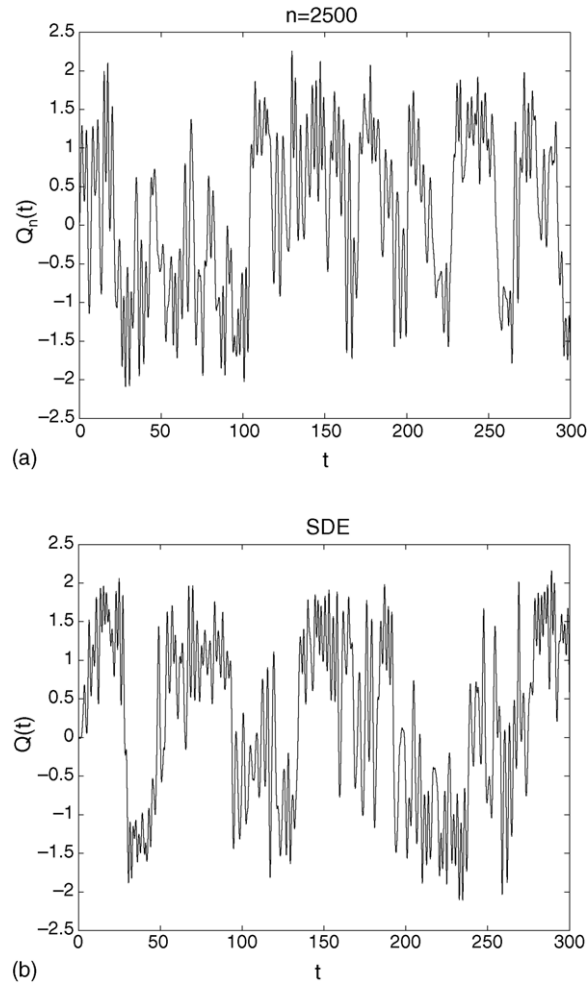


Fig. 11. Left: sample path of $Q_n(t)$ solving the Hamiltonian system for $n = 2500$, $\beta = 1$, and a self potential $V(Q) = (1/4)Q^4 - (1/2)Q^2$. Right: sample path of $Q(t)$ solving the approximating SDE.

4.3. Time series analysis

In this section we analyze long time series for $P_n(t)$, $Q_n(t)$ obtained from a direct numerical simulation of (48), n large, and estimate the parameters α_0 , β_0 , and β in the approximating SDE (50) using MLE. This time series analysis is a generalization of that in Section 2.4. First we discuss the MLE for continuous observations. Given a continuous observation of $\{R(t), P(t)\}$ on $t \in [0, T]$ the maximum likelihood estimates of α_0 and $\mu_0 = \beta\beta_0^{-1}$ satisfy [30]

$$\begin{pmatrix} \int_0^T R^2(t) dt & \int_0^T R(t)P(t) dt \\ \int_0^T R(t)P(t) dt & \int_0^T P^2(t) dt \end{pmatrix} \begin{pmatrix} \hat{\alpha}_0 \\ \hat{\mu}_0 \end{pmatrix} = - \begin{pmatrix} \int_0^T R(t) dR(t) \\ \int_0^T P(t) dR(t) \end{pmatrix}.$$

Formally this may be obtained by using least squares, as in Section 2.4 for the OU process: choose α_0 and μ_0 to minimize the L^2 (in time) norm of the white noise on $(0, T)$. The diffusion coefficient can then be estimated by (23)

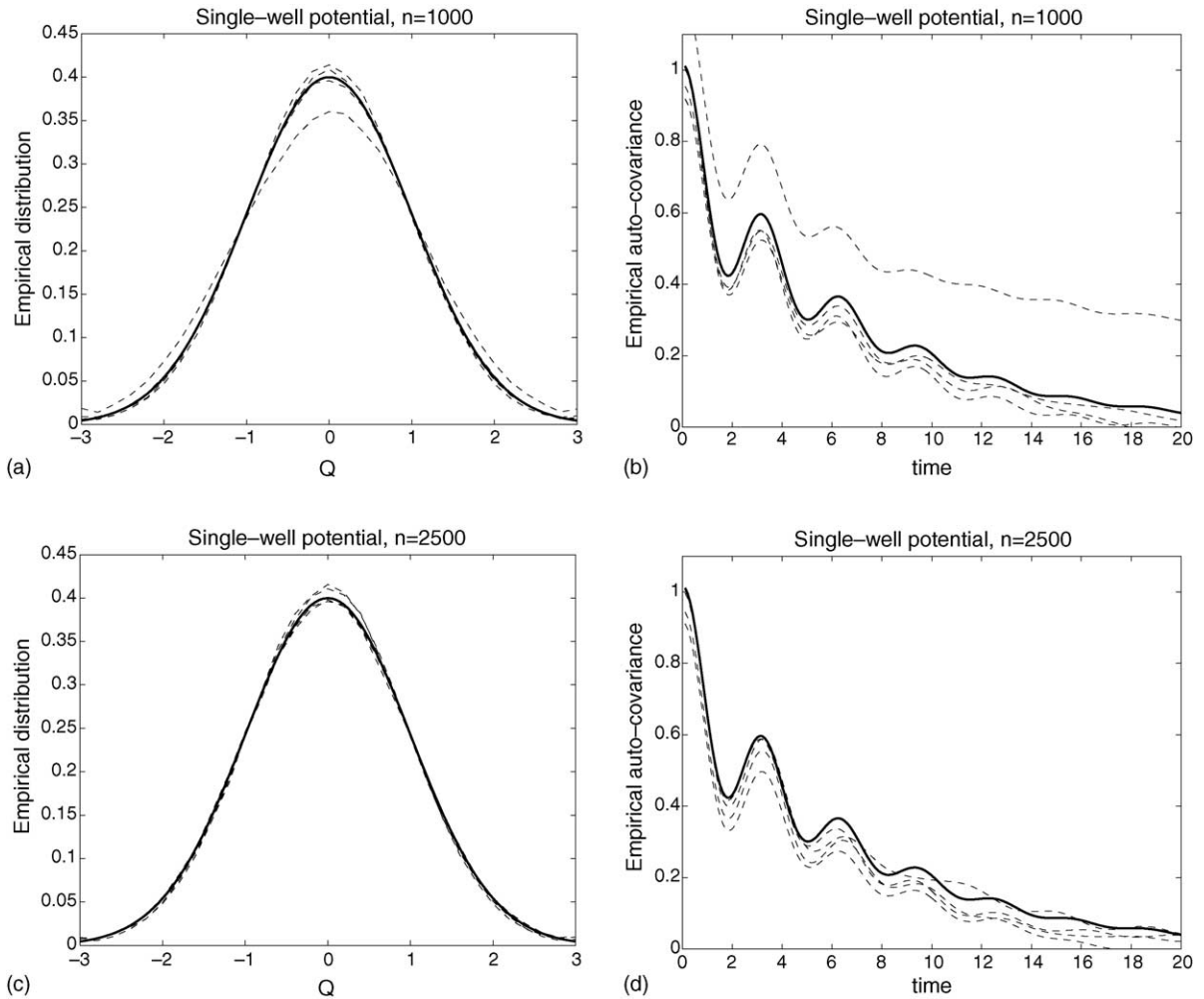


Fig. 12. Left: empirical distribution for four sample path solutions of the Hamiltonian system with a quadratic potential (dashed lines) and the equilibrium distribution for unit temperature (solid line). Right: the empirical auto-covariances for sample path solutions of the Hamiltonian system (dashed lines) and the approximating SDE (solid line). The top figures are for $n = 1000$ and the bottom ones for $n = 2500$. The temperature is $1/\beta = 1$.

with $Y(t)$ replaced by $R(t)$. Also, as in Section 2.4, we require large time intervals to estimate drift parameters, but not to estimate the diffusion coefficient.

To analyze discrete time, we start by rewriting the (Itô) SDE (50) in integral form:

$$\begin{aligned}
 R(t) &= \ddot{Q}(t) + V'(Q(t)), \\
 R(t) &= R(t_0) e^{-\alpha_0(t-t_0)} - \beta\beta_0^{-1} \int_{t_0}^t P(s) e^{-\alpha_0(t-s)} ds + (2\alpha_0\beta_0^{-1})^{1/2} \int_{t_0}^t e^{-\alpha_0(t-s)} dB(s).
 \end{aligned}
 \tag{52}$$

Thus, given a time series of $Q(t)$ the first equation in (52) gives an explicit expression for the auxiliary field $R(t)$. In practice, we compute a discrete times series of $Q(t)$, and calculate, using finite differencing, a discrete time series of $R_j = R(t_j)$, $t_j = j \Delta t$. The finite differencing we use is based on the difference scheme used to solve the Hamiltonian problem itself, so that we actually recover the discrete force applied to the distinguished particle in

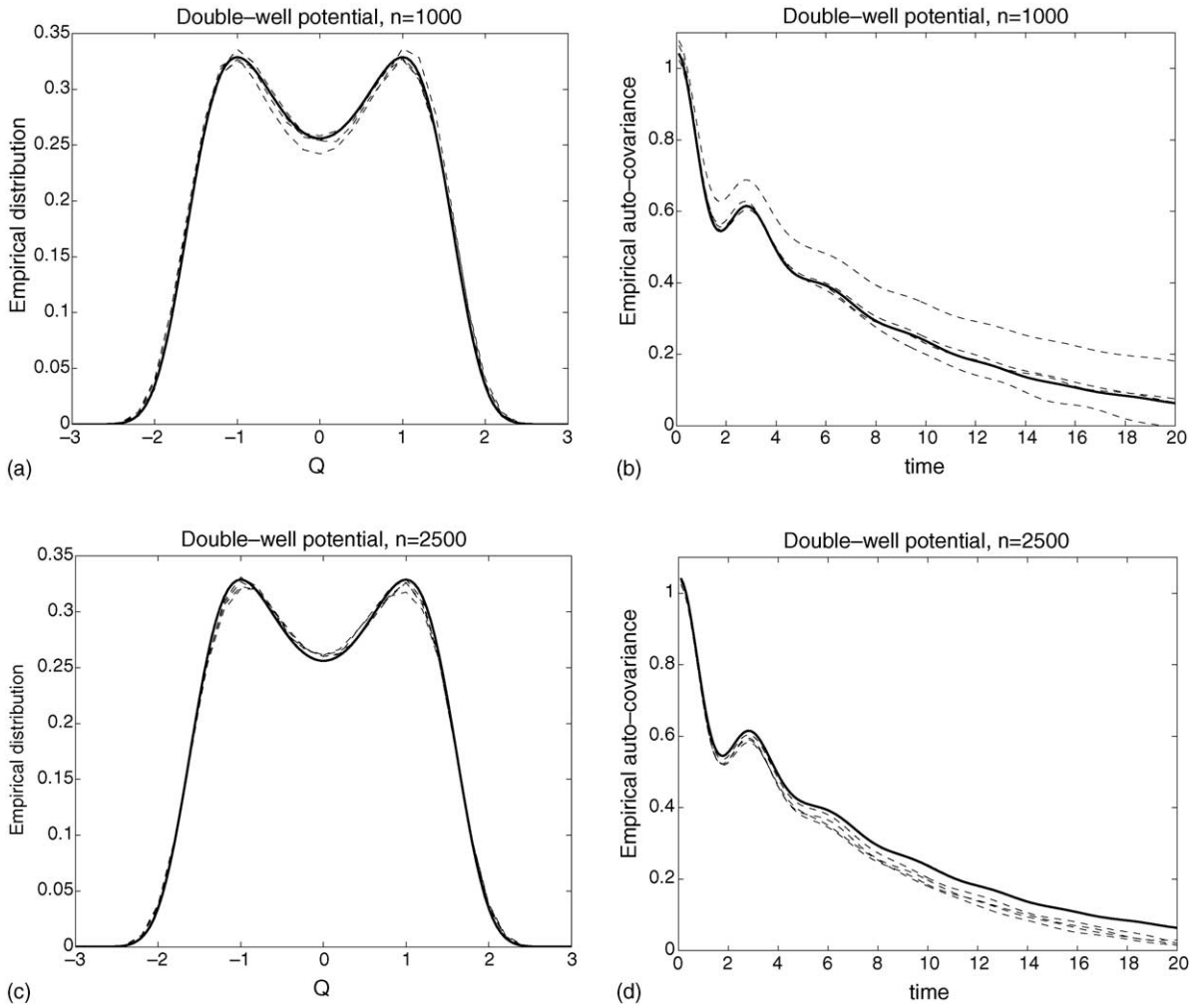


Fig. 13. Same as Fig. 12 for a double-well potential.

the course of the numerical integration. For more complex problems this will not be possible and non-trivial issues arise when performing numerical differentiation to find R from Q and P [30].

The second equation in (52) can then be put in the following discrete form

$$R_{j+1} = \lambda_0 R_j + \mu_0 U_j + Z_{j+1},$$

where

$$U_j = - \int_{t_j}^{t_{j+1}} P(s) e^{-\alpha_0(t_{j+1}-s)} ds, \quad (53)$$

the Z_j are i.i.d. $\mathcal{N}(0, \gamma_0^2)$, and the parameters λ_0 , μ_0 , γ_0 are given by

$$\lambda_0 = e^{-\alpha_0 \Delta t}, \quad \mu_0 = \frac{\beta}{\beta_0}, \quad \gamma_0^2 = \beta_0^{-1} [1 - \exp(-2\alpha_0 \Delta t)]. \quad (54)$$

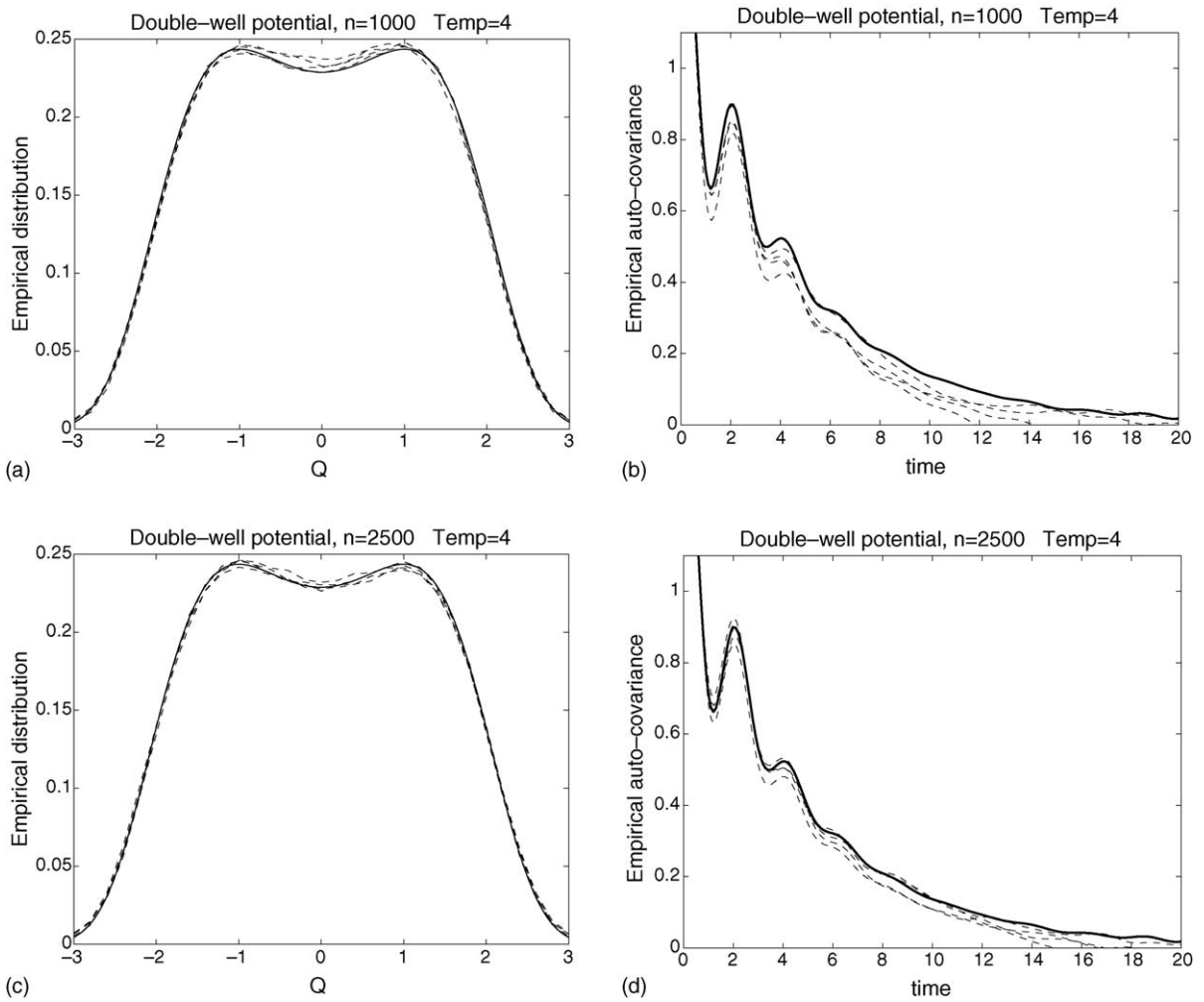


Fig. 14. Same as Fig. 13 for temperature $1/\beta = 4$.

Thus estimates for λ_0 , μ_0 and γ_0 will imply estimates for α_0 , β_0 and β . In practice, the U_j are calculated by approximating the integral (53) by quadrature. In fact, since $P(t)$ is less regular than $Q(t)$, a better numerical approximation is obtained if (53) is first integrated by parts and then quadrature applied to the resulting integral over the path of Q . As in Section 2.4, parameter estimation performs poorly if the sampling rate is too small. Thus $t_{j+1} - t_j$ is large enough that the deviation of U_j from $P(t_j)$ is significant, and the dependence on α_0 must be allowed for.

The likelihood function for the data R_j , given the “input” U_j , is

$$\mathcal{L}(\lambda_0, \mu_0, \gamma_0) = \prod_{j=1}^N \frac{1}{\sqrt{2\pi\gamma_0^2}} \exp \left[-\frac{(R_{j+1} - \lambda_0 R_j - \mu_0 U_j)^2}{2\gamma_0^2} \right].$$

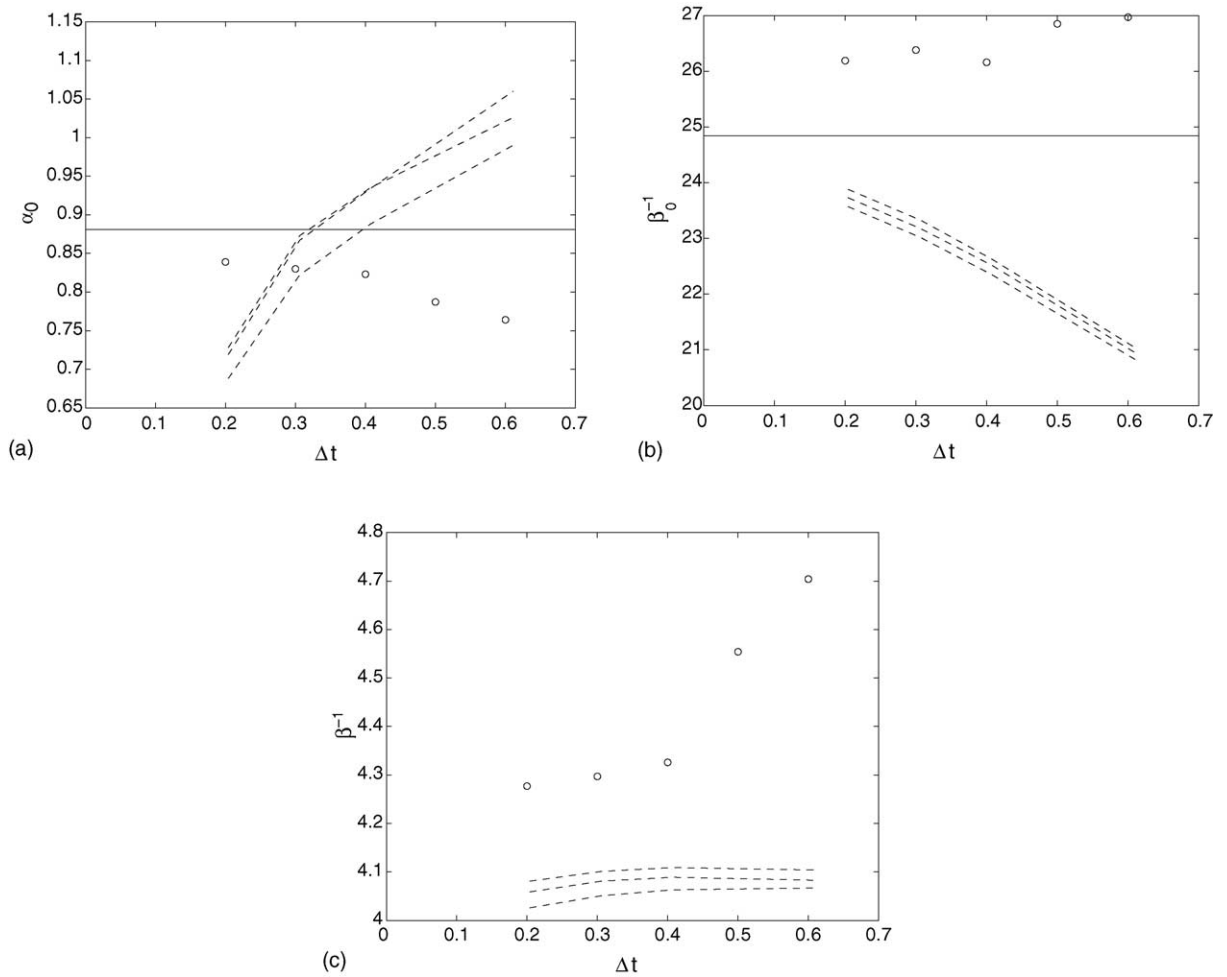


Fig. 15. Estimates of (a) α_0 , (b) β_0^{-1} and (c) β^{-1} vs. the time step Δt . The three dashed lines are estimates based on three sample paths of length 10^5 time units of $Q_n(t)$, $n = 2500$. The open circles are estimates based on a collection of short time series drawn from 20,000 paths of $Q_n(t)$, $n = 20,000$. The solid lines are the estimates based on the results of Section 2.

The parameters λ_0 , γ_0^2 , and μ_0 are estimated by maximizing the log-likelihood function. First, λ_0 and μ_0 are estimated by minimizing numerically the following expression:

$$\sum_{j=1}^N [R_{j+1} - \lambda_0 R_j - \mu_0 U_j(\alpha_0(\lambda_0))]^2.$$

Then, γ_0^2 is obtained by

$$\gamma_0^2 = \frac{1}{N} \sum_j (R_{j+1} - \lambda_0 R_j - \mu_0 U_j(\alpha_0))^2.$$

Inverting (54) we obtain the model parameters:

$$\alpha_0 = -\frac{1}{\Delta t} \log \lambda_0, \quad \beta_0^{-1} = \frac{\gamma_0^2}{1 - \lambda_0^2}, \quad \beta = \beta_0 \mu_0.$$

In Fig. 15 we plot estimates of (a) α_0 , (b) β_0^{-1} and (c) β^{-1} versus the time step Δt , based on time series analyses for three sample paths of $Q_n(t)$ with $n = 2500$, $\beta^{-1} = 4$ and self-potential $V(Q) = (1/2)Q^2$ (dashed lines); the integration interval is 10^5 time units. The open circles represent estimates using a collection of short time series drawn from 20,000 paths of $Q_n(t)$; here $n = 20,000$. The expected values for α_0 and β_0^{-1} , based on the estimates of Section 2, are 0.881 and 24.86, respectively, and are represented in the graphs by horizontal solid lines.

The results show the following:

- (1) For the value $n = 2500$ the agreement between the time series analysis and the linear response theory is fairly good, though discrepancies of the order 5–15% remain.
- (2) The time-averaged and ensemble averaged estimates also show reasonable agreement, but do differ on the order of 5–15%.
- (3) The Δt dependence of the parameter estimates is somewhat different from what we observed in fitting an OU process to sums of oscillators in Section 2.4. The variability with Δt , whilst confined to 5–15%, is plainly visible for *all* Δt used and the plateau effect present in Section 2.4 is not visible. However the spectrum of this nonlinear Hamiltonian problem is more complicated than for the sums of nonlinear oscillators studied earlier and it is possible that nonlinear interaction generates characteristic periods for the oscillators which interfere with the parameter estimation even at the upper end of the sampling rates used in Fig. 15.

In summary, the time series analysis has been shown to be quite successful in fitting SDE models to components of a bath-particle Hamiltonian model of generalized Kac–Zwanzig type. The linear response theory provides some theoretical justification for the form of SDE model that we fit and the numerical experiments show the ability of the SDE model to match behaviour of the Hamiltonian system.

5. Conclusions

Our primary objective in this paper is to understand the approximation of components of large Hamiltonian systems by SDEs. The Kac–Zwanzig models provide an illustration of situations where this may be carried out analytically, using a particle coupled to a heat bath of oscillators via linear Hookean springs, and theorems may be proved [1–3,10]. Here we have generalized this model to allow nonlinear bath-particle coupling. In pursuing our primary objective we have shown the following:

- (1) That weighted sums of n solutions of nonlinear oscillators, with canonical initial data, can behave, for large n , like Gaussian processes. Furthermore, for certain choices of weights, these Gaussian processes are close to OU processes.
- (2) Linear response theory can be used to approximate the force exerted by the heat bath on the distinguished particle. The resulting force splits into a drag (mean force) and noise (fluctuations about the mean). These are related by the fluctuation–dissipation relation and, in the case of linear bath-particle coupling, reduce to a form which is *provably* correct. For the case of nonlinear bath-particle coupling the techniques we use do not lead to a proof, and are somewhat ad hoc. Numerical experiments, however, confirm their validity, especially at high temperatures.

- (3) This linear response approximation, combined with the knowledge that sums of nonlinear oscillators can be well-approximated by OU processes, leads to a conjectured form for the approximation of the particle in a heat bath by an SDE.
- (4) Time series analysis can be used to optimize the parameters of this SDE so that its solutions match those of the particle in the Hamiltonian bath-particle model. The ability of the SDE model to reproduce the projected Hamiltonian dynamics is very good.

The success of the program we have carried out here, culminating in time series analysis to fit an SDE to a partially observed Hamiltonian system, suggests that the idea of Kac–Zwanzig heat bath models can be extended significantly beyond the simple linear bath-particle coupling originally envisioned [1–3,10]. The work presented here is a platform from which more complicated Hamiltonian systems, such as those arising in biomolecular modelling [11], can be analyzed by similar techniques from time series analysis.

Acknowledgements

We are grateful to D. Brillinger, A. Chorin, S. Evans, Y. Farjoun, R. Mannella, J. Neu, Y. Peres, P. Tupper and P. Wiberg for helpful discussions. RK was supported by the Israel Science Foundation founded by the Israel Academy of Sciences and Humanities, by the Alon Fellowship, and by the Applied Mathematical Sciences subprogram of the Office of Energy Research of the US Department of Energy under contract DE-AC03-76-SF00098. A.M.S. was supported by the EPSRC, UK.

Appendix A. Proof of lemmas

Lemma A.1. *Let Y_n and Y be defined as in Theorem 2.1. Then the finite-dimensional distributions of Y_n weakly converge to those of Y .*

Proof. Let $t_1 < t_2 < \dots < t_r$ be a collection of times. We need to show that the r -dimensional vectors with components $Y_n(t_\alpha)$, $\alpha = 1, 2, \dots, r$, weakly converges, as $n \rightarrow \infty$, to a Gaussian vector with mean zero and covariance $\sigma(t_\alpha - t_\beta)$, with $\sigma(t)$ given by (14).

The proof relies on the multivariate Lindeberg–Feller theorem (see [31]; see also [10]). Defining $z_{j,\alpha}^{(n)}$ by

$$z_{j,\alpha}^{(n)} = k_j^{1/4} \xi_j^3 \Phi^3(\xi_j \nu_j t_\alpha + \tau_j),$$

so that

$$Y_n(t_\alpha) = \sum_{j=1}^n z_{j,\alpha}^{(n)},$$

the lemma holds if for all $\alpha, \gamma = 1, 2, \dots, r$,

$$(1) \quad \lim_{n \rightarrow \infty} \sum_{j=1}^n \mathbb{E}[z_{j,\alpha}^{(n)} z_{j,\gamma}^{(n)}] = \lim_{n \rightarrow \infty} \sigma_n(t_\alpha - t_\gamma) = \sigma(t_\alpha - t_\gamma).$$

(2) For all $\epsilon > 0$:

$$\lim_{n \rightarrow \infty} \sum_{j=1}^n \mathbb{E} \left(|z_{j,\alpha}^{(n)} z_{j,\gamma}^{(n)}|; \sum_{\delta=1}^r |z_{j,\delta}^{(n)}| > \epsilon \right) = 0,$$

where $\mathbb{E}(f; A)$ denotes the integral of f over the set A .

We start with the first condition of the Lindeberg–Feller theorem. The finite- n auto-covariance $\sigma_n(t)$ is given by (17). By our choice of the v_j , the boundedness $h(t)$:

$$|h(t)| \leq \frac{1}{\sqrt{2}\Gamma(3/4)} \int_{-\infty}^{\infty} \xi^8 e^{-\xi^4/4} d\xi = \frac{8\Gamma(9/4)}{\Gamma(3/4)},$$

the continuity of $h(t)$, and the assumptions on $g(v)$, it follows that

$$\lim_{\delta \rightarrow \infty} \sigma_n(t_\alpha - t_\gamma) = \beta^{-3/2} \int_0^\infty g(v) h(\beta^{-1/4} v(t_\alpha - t_\gamma)) dv = \sigma(t_\alpha - t_\gamma).$$

For the second condition of the Lindeberg–Feller theorem we note that

$$|z_{j,\alpha}^{(n)} z_{j,\gamma}^{(n)}| \leq \frac{1}{2} k_j^{1/2} \xi_j^6$$

and that

$$\sum_{\delta=1}^r |z_{j,\delta}^{(n)}| > \epsilon \quad \text{only if} \quad \sum_{\delta=1}^r \frac{1}{\sqrt{2}} k_j^{1/4} |\xi_j|^3 > \epsilon.$$

It follows that

$$\mathbb{E} \left(|z_{j,\alpha}^{(n)} z_{j,\gamma}^{(n)}|; \sum_{\delta=1}^r |z_{j,\delta}^{(n)}| > \epsilon \right) \leq \frac{\beta^{3/4} k_j^{1/2}}{2} \int_{r/\sqrt{2} k_j^{1/4} |\xi|^3 > \epsilon} \xi^8 e^{-\beta \xi^4/4} d\xi.$$

Since $k_j^{1/4} \leq C(\Delta v)^{1/2} = Cn^{(a-1)/2}$, then the right hand side decays exponentially fast as $n \rightarrow \infty$, independently of j . Summation over $j = 1, \dots, n$ still yields an exponentially decaying quantity. This completes the proof. \square

Lemma A.2. *Let Y_n be defined as in Theorem 2.1. Then there exist positive constants α, η, M such that for all n*

$$\mathbb{E}|Y_n(t+u) - Y_n(t)|^\alpha \leq M|u|^{1+\eta}.$$

Proof. Since $Y_n(t)$ is a stationary process, it is sufficient to verify that there exist $\alpha, \eta, M > 0$, such that

$$\mathbb{E}|Y_n(t) - Y_n(0)|^\alpha \leq M|t|^{1+\eta}.$$

Let $\eta > 0$ be given and take $\alpha = 2p$, where $p > 2$ is an integer sufficiently large so that

$$\gamma = \frac{1 + \eta}{2p} \in \left(0, \frac{b}{2}\right)$$

and b is the constant associated with the decay rate of $g(v)$.

Now:

$$\mathbb{E}|Y_n(t) - Y_n(0)|^{2p} = \mathbb{E} \left| \sum_{j=1}^n k_j^{1/4} \xi_j^3 [\Phi^3(\xi_j v_j t + \tau_j) - \Phi^3(\tau_j)] \right|^{2p} \equiv \mathbb{E} \left| \sum_{j=1}^n \Psi_j \right|^{2p},$$

which can be expanded as a sum of $(2p)^n$ terms:

$$\mathbb{E}|Y_n(t) - Y_n(0)|^{2p} = \sum_{j_1=1}^n \cdots \sum_{j_{2p}=1}^n \mathbb{E}[\Psi_{j_1} \Psi_{j_2} \cdots \Psi_{j_{2p}}]. \tag{A.1}$$

Note that the Ψ_j are mutually independent variables that have mean zero. Hence, all the summands in (A.1) that have an index j_ℓ that appears only once vanish.

We regroup the summation (A.1) by the “pattern” of repeated indices. A pattern is an r -tuple, $\{p_1, p_2, \dots, p_r\}$, $p_1 \geq p_2 \geq \dots \geq p_r$, meaning that a certain index repeats p_1 times, another index repeats p_2 times, and so on up to r . Clearly, all the p_ℓ satisfy $2 \leq p_\ell \leq 2p$, $p_1 + p_2 + \dots + p_r = 2p$, and the number r of distinct indices varies between 1 and p (if r were larger than p there would be an index that appears only once). With each pattern $\{p_1, p_2, \dots, p_r\}$ is associated a combinatorial constant, C_{p_1, p_2, \dots, p_r} , which is the number of possible arrangements of the pattern. We do not calculate these constants, but note that

$$\sum_{\{p_1, \dots, p_r\}} C_{p_1, \dots, p_r}$$

can be bounded by a constant that depends only on p ; constants that depend on p (and not on n) will be denoted generically by C_p . (For example, if $p = 2$ then the only patterns are $\{4\}$ and $\{2, 2\}$, with combinatorial factors $C_4 = 1$ and $C_{2,2} = 3$.)

Each pattern consists of r distinct indices, and therefore can be “decoded” in

$$\binom{n}{r}$$

different ways by assigning an index $1, 2, \dots, n$ to each of the distinct j_ℓ in (A.1). A simple upper bound on (A.1) is obtained by letting all r indices run over $1, 2, \dots, n$, so that

$$\mathbb{E}|Y_n(t) - Y_n(0)|^{2p} \leq \sum_{\{p_1, \dots, p_r\}} C_{p_1, \dots, p_r} \sum_{j_1=1}^n \mathbb{E}|\Psi_{j_1}|^{p_1} \cdots \sum_{j_r=1}^n \mathbb{E}|\Psi_{j_r}|^{p_r}. \tag{A.2}$$

We then use the fact that for all $\gamma < 1$ there exists a constant K_γ such that

$$|\Phi^3(s) - \Phi^3(0)| \leq K_\gamma |s|^\gamma$$

to deduce that

$$\mathbb{E}|\Psi_{j_\ell}|^{p_\ell} \leq K_\gamma^{p_\ell} k_{j_\ell}^{p_\ell/4} v_{j_\ell}^{\gamma p_\ell} |t|^{\gamma p_\ell} \mathbb{E}|\xi_{j_\ell}^{(3+\gamma)p_\ell}| = C_p g^{p_\ell/2} (v_{j_\ell}) v_{j_\ell}^{\gamma p_\ell} \Delta v^{p_\ell/2} |t|^{\gamma p_\ell} \leq C_p v_{j_\ell}^{(\gamma-(1+b)/2)p_\ell} \Delta v^{p_\ell/2} |t|^{\gamma p_\ell},$$

where we have used the assumed bound on $g(v)$. Substituting the latter inequality into (A.2) we get

$$\mathbb{E}|Y_n(t) - Y_n(0)|^{2p} \leq C_p |t|^{2\gamma p} \sum_{\{p_1, \dots, p_r\}} C_{p_1, \dots, p_r} \Delta v^{p-r} \prod_{\ell=1}^r \sum_{j_\ell=1}^n v_{j_\ell}^{(\gamma-(1+b)/2)p_\ell} \Delta v.$$

Because each p_ℓ is greater or equal to 2 and by our choice of γ , each of the sums over j_ℓ converges as $n \rightarrow \infty$, and therefore the finite- n sums can be uniformly bounded, yielding

$$\mathbb{E}|Y_n(t) - Y_n(0)|^{2p} \leq C_p |t|^{2\gamma p} = C_p |t|^{1+\eta}.$$

This completes the proof. □

References

- [1] G. Ford, M. Kac, P. Mazur, Statistical mechanics of assemblies of coupled oscillators, *J. Math. Phys.* 6 (1965) 504–515.
- [2] G. Ford, M. Kac, On the quantum Langevin equation, *J. Stat. Phys.* 46 (1987) 803–810.
- [3] R. Zwanzig, Nonlinear generalized Langevin equations, *J. Stat. Phys.* 9 (1973) 215–220.
- [4] A. Stuart, J. Warren, Analysis and experiments for a computational model of a heat bath, *J. Stat. Phys.* 97 (1999) 687–723.
- [5] B. Cano, A. Stuart, Under-resolved simulations of heat baths, *J. Comp. Phys.* 169 (2001) 193–214.
- [6] O. Hald, R. Kupferman, Asymptotic and numerical analyses for mechanical models of heat baths, *J. Stat. Phys.* 106 (2002) 1121–1184.
- [7] A. Chorin, A. Kast, R. Kupferman, Optimal prediction of underresolved dynamics, *Proc. Natl. Acad. Sci. USA* 95 (1998) 4094–4098.
- [8] A. Kast, Optimal prediction of stiff oscillatory mechanics, *Proc. Natl. Acad. Sci. USA* 97 (2000) 6253–6257.
- [9] W. Huisinga, C. Schütte, A. Stuart, Extracting macroscopic stochastic dynamics: model problems, *Commun. Pure Appl. Math.* 56 (2003) 234–269.
- [10] R. Kupferman, A. Stuart, J. Terry, P. Tupper, Long term behaviour of large mechanical systems with random initial data, *Stoch. Dyn.* 2 (2002) 533–562.
- [11] H. Grubmüller, P. Tavan, Molecular dynamics of conformational substrates for a simplified protein model, *J. Chem. Phys.* 101 (1994) 5047–5057.
- [12] A. Majda, I. Timofeyev, E. Vanden-Eijnden, A priori tests of a stochastic mode reduction strategy, *Physica D* 170 (2002) 206–252.
- [13] P. Billingsley, *Convergence of Probability Measures*, 2nd ed., Wiley, New York, 1999.
- [14] M. Bianucci, R. Mannella, B. West, P. Grigolini, From dynamics to thermodynamics: linear response and statistical mechanics, *Phys. Rev. E* 51 (1995) 3002–3022.
- [15] M. Bianucci, R. Mannella, Linear response of Hamiltonian chaotic systems as a function of the number of degrees of freedom, *Phys. Rev. Lett.* 77 (1996) 1258–1261.
- [16] E. Cortes, B. West, K. Lindenberg, On the generalized Langevin equation: classical and quantum mechanical, *J. Chem. Phys.* 82 (1985) 2708–2717.
- [17] S. Habib, H. Kandrup, Nonlinear noise in cosmology, *Phys. Rev. D* 46 (1992) 5303–5314.
- [18] K. Lindenberg, V. Seshadri, Dissipative contributions of internal multiplicative noise. I. Mechanical oscillator, *Physica A* 109 (1981) 483–499.
- [19] T. Brun, Quasiclassical equations of motion for nonlinear Brownian systems, *Phys. Rev. D* 47 (1993) 3383–3393.
- [20] B. Hu, J. Paz, Y. Zhang, Quantum Brownian motion in a general environment. II. Nonlinear coupling and perturbative approach, *Phys. Rev. D* 47 (1993) 1576–1594.
- [21] M. Abramowitz, I. Stegun, *Handbook of Mathematical Functions with Formulas, Graphs and Mathematical Tables*, Dover, New York, 1971.
- [22] I. Gikhman, A. Skorokhod, *Introduction to the Theory of Random Processes*, Dover, Mineola, NY, 1996.
- [23] A. Majda, I. Timofeyev, Remarkable statistical behavior for truncated Burgers–Hopf dynamics, *Proc. Natl. Acad. Sci. USA* 97 (2000) 12413–12417.

- [24] P. Kloeden, E. Platen, *Numerical Solution of Stochastic Differential Equations*, Springer-Verlag, Berlin, 1992.
- [25] B.P. Rao, *Statistical Inference for Diffusion Type Processes*, Arnold, London, 1999.
- [26] P. Brockwell, R. Davis, *Time Series: Theory and Methods*, 2nd ed., Springer-Verlag, New York, 1991.
- [27] H. Goldstein, C. Poole, J. Safko, *Classical Mechanics*, 3rd ed., Prentice-Hall, 2002.
- [28] D. Evans, G. Morriss, *Statistical Mechanics of Nonequilibrium Liquids*, Academic Press, London, 1990.
- [29] R. Kupferman, Fractional kinetics in Kac–Zwanzig heat bath models, *J. Stat. Phys.* 114 (2004) 291–326.
- [30] A. Stuart, P. Wiberg, Parameter estimation for partially observed hypo-elliptic diffusions, *Journal of the Royal Statistical Society, Series B*, submitted.
- [31] A. Dvoretzky, Asymptotic normality of sums of dependent random vectors, in: *Proceedings of the Fourth International Symposium on Multivariate Analysis IV*, Dayton, OH, 1975, North-Holland, Amsterdam, 1977, pp. 23–34.